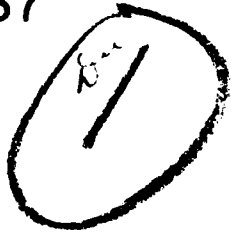


AD 741717

NAVY N6⁹2306-69-C-0261
NSF GA 19937



A DIAGNOSTIC STUDY OF THE PLANETARY BOUNDARY LAYER OVER THE OCEANS

BY

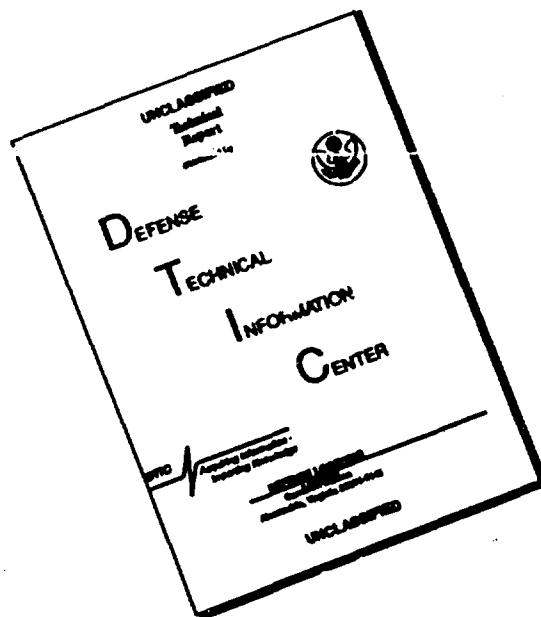
WILLIAM M. GRAY

D D C
RECEIVED
APR 13 1972
B



Reproduced by
NATIONAL TECHNICAL
INFORMATION SERVICE
Springfield, Va. 22151

DISCLAIMER NOTICE



THIS DOCUMENT IS BEST QUALITY AVAILABLE. THE COPY FURNISHED TO DTIC CONTAINED A SIGNIFICANT NUMBER OF PAGES WHICH DO NOT REPRODUCE LEGIBLY.

DIAGNOSTIC STUDY OF THE PLANETARY BOUNDARY LAYER
OVER THE OCEANS

by

William M. Gray

Preparation of this report

has been supported by

U.S. Navy Weather Research Facility
N62306-69-C-0261

NSF Grant GA 19937

Department of Atmospheric Science

Colorado State University

Fort Collins, Colorado

February 1972

Atmospheric Science Paper No. 179

TABLE OF CONTENTS

		<u>Page</u>
	Abstract	iv
I.	BACKGROUND	1
	Previous Observational Studies	2
	Use of Rawin and Pibal Observations	4
	How Much p.b.l. Wind Veering Is There over the Oceans?	5
II.	OBSERVATIONAL CONSIDERATIONS	6
	Veering Variations	6
	Ship Wind Restrictions	11
	Other Complications	11
	Stability Variations	12
	Horizontal Temperature Gradient Variations	14
	Summary	17
III.	DATA SAMPLE	18
	Islands and Atolls Data	18
	80,000 Ocean Ship Veering Reports from 1949-1964	18
IV.	WIND VEERING AT ISLANDS AND ATOLLS	30
	Individual Station Long Term Veering	30
	Individual Station Mean Monthly Veering	30
	Veering Information from West Pacific and West Indies	36
	Cloud Cluster vs. Clear Area Veering	36
V.	ANGLE VEERING FROM OCEAN SHIPS	39
	Veering vs. Latitude	39
	Veering vs. Wind Direction and Latitude	43
	Veering vs. Wind Speed and Latitude	43
	Veering vs. Season and Latitude	49
	Conclusion	50
VI.	DYNAMIC CONSIDERATIONS	56
	Wind Speeds	56
	Stress Determinations	56

	Surface Ageostrophic Wind Components	61
	Boundary Layer Acceleration for Zero Stress at 1 km. .	64
	Kinetic Energy Dissipation-Generation for Zero Stress at 1 km.	64
	Model of Zero Turbulent Stress at 2 km (\sim 800 mb.) .	70
	Ocean vs. Land Frictional Veering	75
	Estimated Viscosity Coefficient	75
VII.	DISCUSSION	76
	Conceptual View of Oceanic Planetary Boundary Layer .	78
	Required Downward Transport from Higher Levels . . .	79
	Depth of the Boundary Layer	81
	Importance of Oceanic Boundary-Layer Frictional Veer- ing and Relation to CISK Mechanism	87
	Importance of Frictionally-forced Convergence	88
	Further Work	90
	Acknowledgements	91
	Bibliography	92

ABSTRACT

A statistical survey of the wind veering in the lowest two kilometers is made for the oceans of the Northern Hemisphere. The data sample consists of over 100,000 pilot and rawin soundings. This includes observations made from ships in the 0° - 70° latitude belt and observations at atolls and small islands in the 5° - 35° latitude belt. The wind veering is stratified by latitude, season, wind direction and wind speed. The results show average veering values of 8-12 degrees in the lowest km layer and 0-3 degrees in the second km layer. The average veering shows little latitude or seasonal variation. The veering increases with wind speed in the middle latitudes but not in the tropics. As expected from thermal wind considerations, south winds show a characteristic veering of 20° more than north winds. This thermal wind influence is largely eliminated by assuming constancy of thermal wind with height and subtracting the second km layer veering from the first.

It is observed that the height of the planetary boundary layer does not increase towards the equator and can be specified by vertical stability and turbulent intensity considerations without resort to rotation arguments. The frictional induced kinetic energy (KE) dissipation is substantially greater than the cross isobaric KE generation. In the tropics the dissipation to generation ratio is more than five to one. The oceanic boundary layer can be maintained only by a downward transport of KE from higher levels.

I. BACKGROUND

Few meteorologists doubt the crucial importance of the planetary boundary layer (p.b.l.) in atmospheric dynamics. Indeed, a large portion of the Stockholm GARP Report (1967) was devoted to discussions of the planetary boundary layer (p.b.l.) by Charnock and Ellison, Blackadar, Monin and Zilitinkenich, and Priestly. Sheppard (1969) has given a summary of our present p.b.l. knowledge with regard to large scale global modeling.

The associations of cumulus convection with positive p.b.l. relative vorticity is very evident along fronts and on the cyclonic shearing side of the trade winds. This cumulus convection is thought to be primarily induced by frictional wind veering in the p.b.l. Where tropospheric vertical wind shears are small, and other conditions are favorable non-linear feedbacks and flow intensification can occur. This is the so-called CISK* mechanism which is generally believed necessary for the intensification of tropical storms and cloud clusters. Over the oceans the top of the p.b.l. (or where the surface induced mechanical wind veering stops) is observed to be close to the base of the cumulus clouds. These oceanic cumuli are dependent on sub-cloud layer convergence, a significant portion of which is believed to be mechanically forced by surface friction.

The assumptions of the Ekman theory (1905) for this layer (steady

*Conditional Instability of the Second Kind (CISK). Physical idea proposed by Ooyama (1964) and Charney and Eliassen (1964) and so much discussed in connection with the GARP and GATE experiment.

motion, no advection, neutral stability, no thermal wind and constant coefficient of viscosity) are almost never simultaneously valid. The question is, how invalid are these assumptions in the real atmosphere? How much does the so-called "Ekman Layer" of the real atmosphere subscribe to Ekman's theory? Granted that Ekman's theory fails for the individual sounding, nevertheless, is the concept a useful one in a statistical sense where the thermal wind, stability, advection, and tendency variations are mostly averaged out of the data sample?

Turbulence theory is not developed to the point of allowing for a practical, objective, generalized p.b.l. model which will handle all of the parameter variations of the individual time periods in terms of a synoptic-scale data sample. Yet future global numerical forecasting will not be very successful unless a realistic treatment of the p.b.l. is accomplished. Probably we will not be able to wait for a satisfactory turbulence theory to be developed before we proceed in our attempts to parameterize the effects of the p.b.l. in terms of the larger-scale motions. For these reasons the author feels that at this stage our knowledge of the p.b.l. will be most rapidly increased by going directly to the observations and studying empirically how all of the measurable parameters vary.

Previous Observational Studies. Most boundary layer research has concentrated on the lowest 10 to 20 meters of the atmosphere. Thousands of papers have been published on this lowest atmospheric layer. In a comparative sense, the 10 meter to 1 km or Ekman layer has been largely

neglected--especially observationally.

Previous observational studies of the entire p. b. l. frictional veering layer have, in general, been limited in location and/or length of record. Some of these noteworthy pioneering observational studies of the p. b. l. include:

Gregg (1922) - 4 Kite locations over the U.S. (discussed and reworked by Johnson, 1962).

Westwater (1943) - North Sea and Trade Winds

Frost (1948) - A number of locations in Europe.

Gordon (1950a, 1950b, 1952a, 1952b) - North Atlantic

Sheppard, Charnock, and Francis (1952) - Scilly Islands

Sheppard and Omar (1952) - Trades

Charnock, Francis, and Sheppard (1956) - Anegada, Virgin Islands

The latter three studies made use of multi-theodolite observations to obtain higher wind accuracy. This often allowed an estimate of wind component correlations, stress, and exchange coefficients, etc. which contributed to a much better layer description.

The most extensive observational work on the p. b. l. has been accomplished by the University of Wisconsin group led by H. Lettau [Lettau and Davidson (1957), Lettau (1959), Lettau et al. (1962), Lettau (1967), B. Lettau (1967), plus many other papers] and his most active former colleague E. Kung [1963, 1967, 1968, and other papers]. Other recent very worthy observational p. b. l. studies have been accomplished by Findlater et al. (1966), Mendenhall (1967), Bonner and Smith (1967), Clark (1970), Janota (1971), and Cattle (1972).

Additional recent observational studies which have dealt with the p. b. l. have included the work of Atkinson and Saddler (1971), Hasse (1970), Hasse and Wagner (1971), Estoque (1970), Aagaard (1969), Angell et al. (1968), and Kraus (1966). These are about all the researchers who have made significant detailed observational studies through the entire p. b. l.

Most of these later studies have been directed to specific p. b. l. physical questions and have been, of necessity, restrictive in areal extent or time sample. Some of these observations were taken over land. A general deficiency exists with regard to oceanic observations.

With recent availability of magnetic data tape storage at the National Climatic Center, Asheville, N.C., many of these observational deficiencies over the oceans can now be alleviated.

Use of Rawin and Pibal Observations. In order to remove data sample restrictions and obtain a broader view of the p. b. l., both pibal and rawinsonde data are used in the present study. The use of conventional pibal and rawinsonde data solves the problem of spatial representation. These observations are routinely available from widely separated locations having many different environmental characteristics. The more accurate but much less abundant special observations are not used (except for a small amount of 1967 Line Island Experiment data - Madden, et al. 1971). A sacrifice of individual site representativeness for a large data sample is felt justified by the fact that it is the average, broader-scale, p. b. l. effects which are being sought. A large data sample is more likely to be of value for this purpose than a highly accurate data

sample which may have biases characteristic of the individual site thermal wind, stability, etc. Additional observational restrictions include limited vertical resolution and real turbulent fluctuations. The author feels that these latter fluctuations are largely random and are eliminated in a large data sample.

How Much p. b. l. Wind Veering Is There over the Oceans? Some meteorologists say that the Ekman wind veering over the oceans is typically too small to be of much importance and that consequently, the CISK or low-level frictional forcing idea may be overemphasized (Simpson, 1971). In a study of the Trades of the northeast Pacific, Riehl et al. (1951) obtained a mean p. b. l. wind veering of only 4° - 6° . What is the typical frictional wind veering over the oceans? Many other fundamental questions on the oceanic p. b. l. such as its typical height, the change of height as one approaches the equator, the typical momentum and kinetic energy dissipation to generation ratios, etc., remain to be answered.

Let us first compute the frictional veering through the lowest few kilometers at many global locations and under a variety of conditions before we attempt to develop a generalized theory or working model of the p. b. l.

II. OBSERVATIONAL CONSIDERATIONS

Veering Variations. The turbulent nature of the p.b.l. limits the information that can be gained about the broader-scale flow from individual observations. Mechanical eddies on gust scales of 50-500 m can often disrupt the upward trajectory of the balloon and typically give individual veering values unrepresentative of the average veering conditions surrounding the ascent location. Careful double or triple theodolite observations often cannot overcome this turbulence induced deficiency of individual observations. In addition, instrumental inaccuracies occur due to initial balloon tracking pickup from ground release and the long time averaging interval (1 to 2 minutes). Extraneous balloon motions can further detract from the representativeness of the individual reports.

Figs. 1 and 2 illustrate the large 6 and 12 hourly 1 km veering fluctuations at Weather Ship N (30°N , 140°W) and at Swan Island (17°N , 84°W). These are typical of all stations. One might have expected a time-series of wind veering in the planetary boundary layer to show some degree of constancy, especially in the relatively steady trade-wind regime. This is not the case. Observed wind veering is highly variable. Figs. 3 and 4 show a typical group of consecutive rawin profiles of vertical variation of wind direction at Wake (20°N , 166°E) and Swan Island (17°N , 84°W). The usual autocorrelogram of lowest km wind veering angle for increasing time lag is shown in Fig. 5. At 6 hours the autocorrelation is ~ 0.3 , at 12 hours and beyond it is \sim zero. Fig. 6

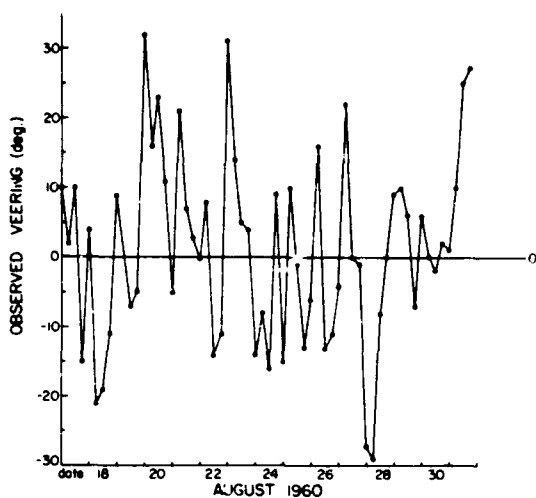
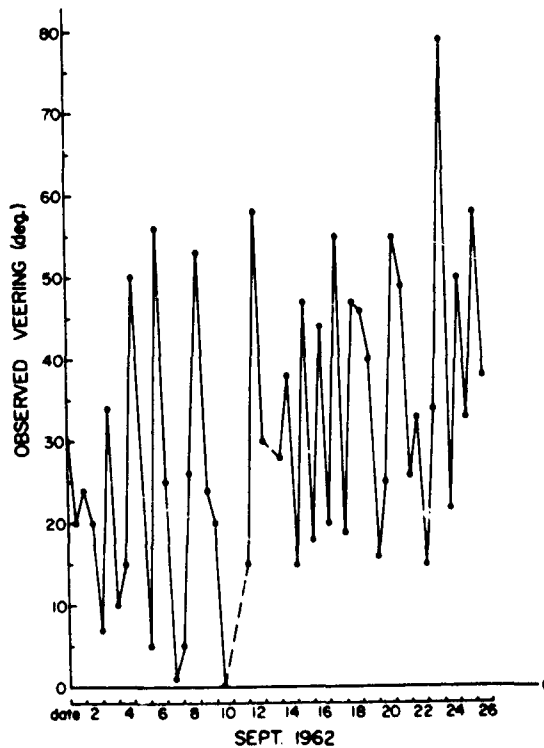
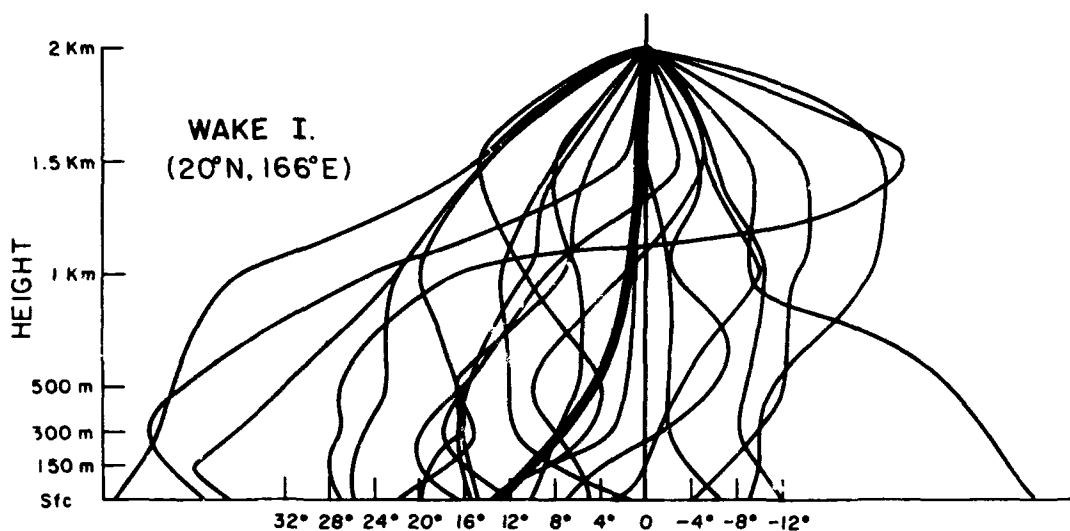


Fig. 1.

Time-series of observed wind veering in lowest km layer at Ship N (30N, 140W) obtained from 6-hourly rawin soundings (from Mendenhall, 1967).

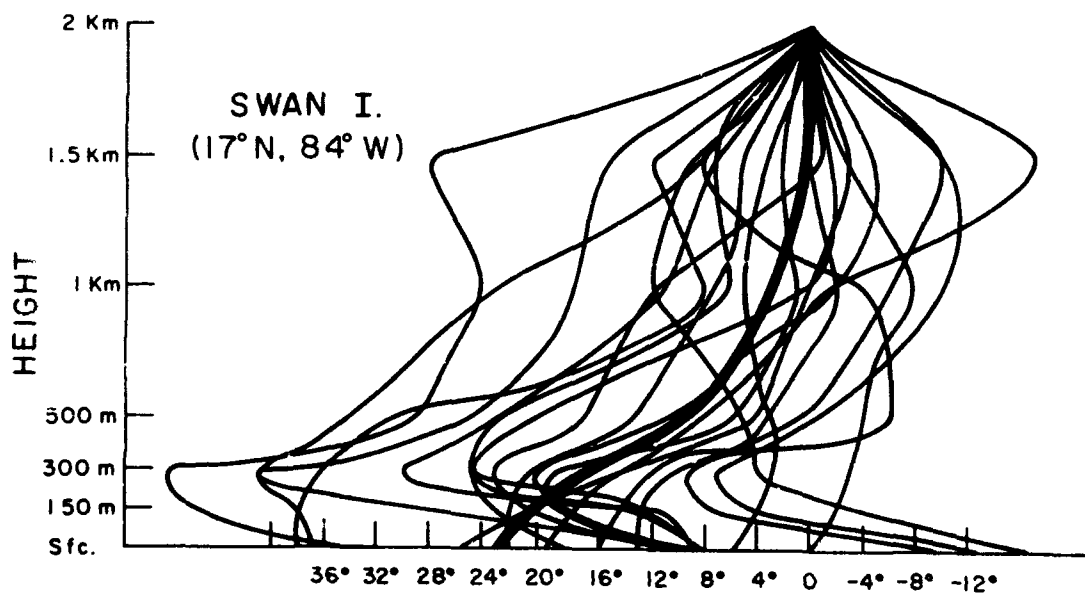
Fig. 2.
Time-series of observed wind veering in lowest km layer at Swan Island (17N, 71W) obtained from 12-hourly rawin soundings. Dashed lines indicate periods of missing observations (from Mendenhall, 1967).





WIND VEERING RELATIVE TO 2 Km. HEIGHT

Fig. 3. Typical individual sounding variation of rawin measured wind direction in lowest 2 km layer. Soundings were taken 6 hours apart. Mean veering shown by the solid line.



WIND VEERING RELATIVE TO 2 Km HEIGHT

Fig. 4. Same as Fig. 3.

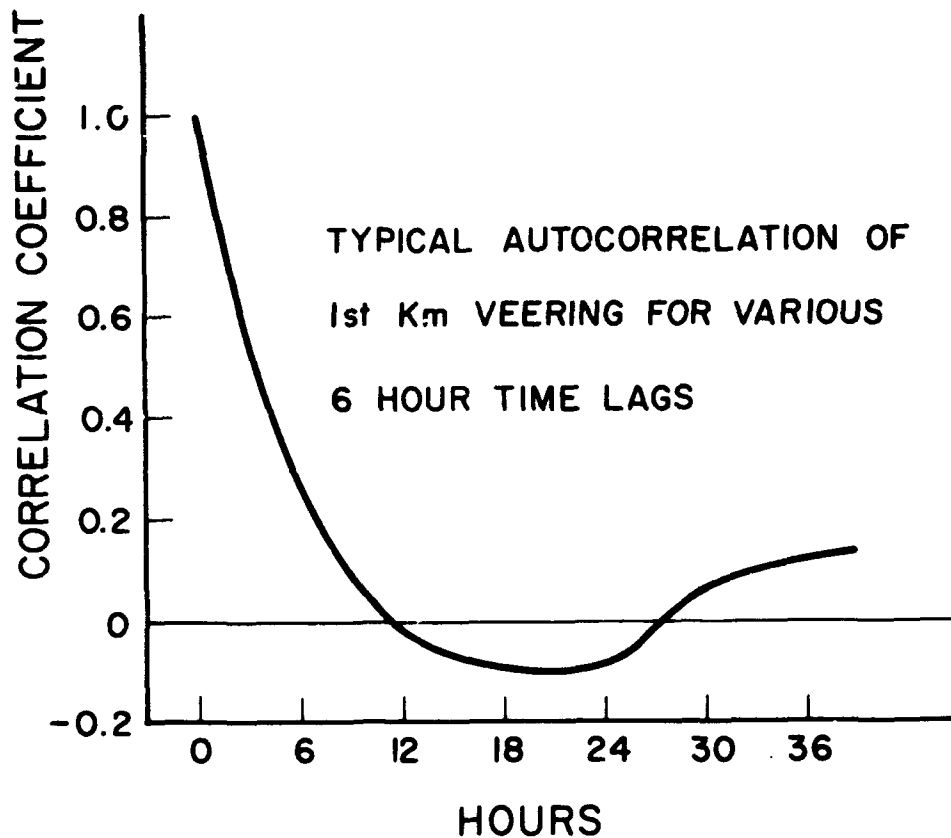
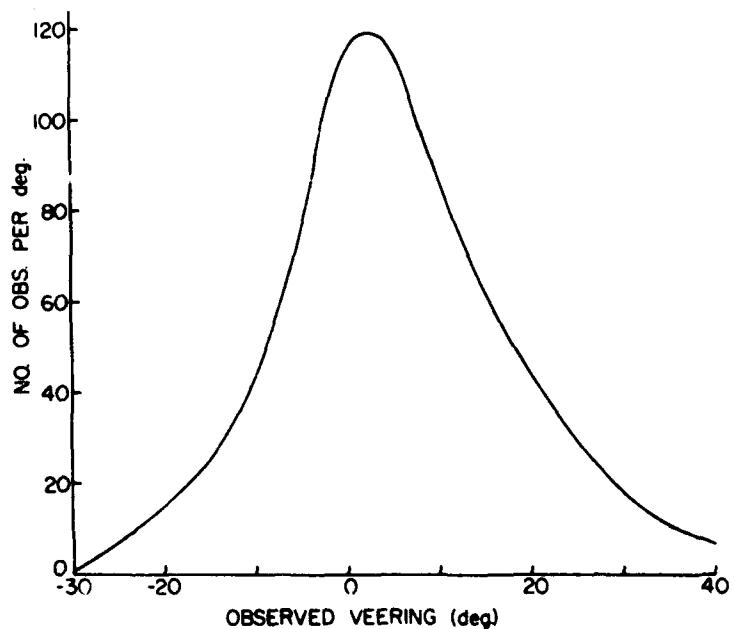


Fig. 5.

Fig. 6.
Smoothed frequency
distribution of veer-
ing at Johnston Island
in the layer from sur-
face to 900 mb. Sample
size: 3696 observations
(from Mendenhall, 1967).



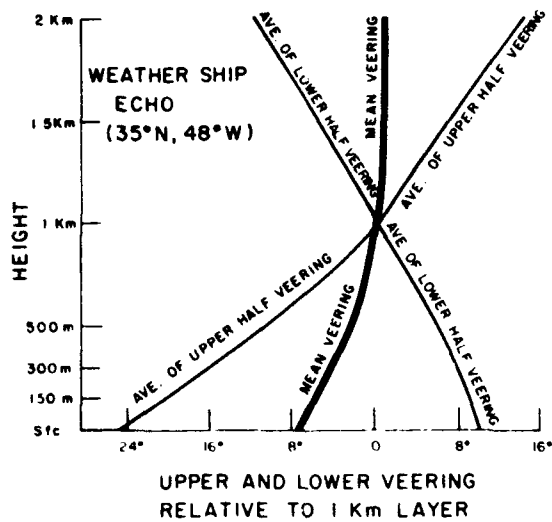


Fig. 7. Average of the 50 percent largest (or upper half) and 50 percent smallest (or lower half) veering values in each of the 1st and 2nd km layer. One km wind is used as reference, heavy line is the mean of all data. Veering is present if the angle shown on the abscissa decrease with height.

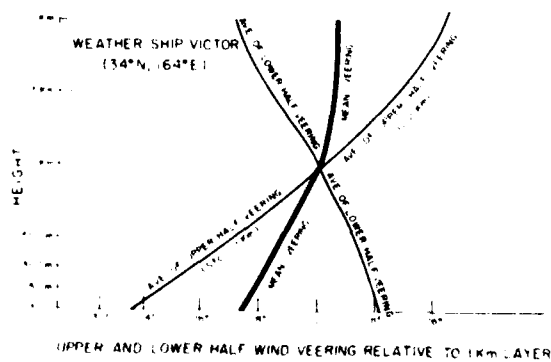


Fig. 8. Same as Fig. 7 for weather ship V.

shows the broad frequency distribution of 1st km wind veering at Johnston Island. This is the normal situation at all stations. This veering is due to both turbulent eddies and random instrumental errors.

These large 1st km veering fluctuations are also present to nearly the same degree in the second km layer as seen in Figs. 7 and 8. Here the veering data was ordered from highest to lowest value in each layer. These figures show the average of the 50 percent largest (or upper half) and 50 percent smallest (or lower half) veering values in each of the 1st and 2nd km layers. The one km wind is used as reference. Veering is present if the angle shown on the abscissa decreases with height. Although one finds a similar scatter of veering in both layers, the average 1st km veering is about 10° more than the 2nd km veering. Turbulent component correlations must be higher in the 1st km. There is no indication that the 2nd km turbulent and instrumental fluctuations are not random. They are self cancelling in a long period average.

Ship Wind Restrictions. Wind directions are least accurate at very light speeds. Wind speeds are least accurate at very strong speeds. Ship soundings are considered less reliable with elevation angles above 60° or below 15° , which are equivalent to average wind speeds of $2\frac{1}{2}$ and 19 m/sec respectively assuming 300 m/min rate of rise. Only a small percent of the wind speeds were below $2\frac{1}{2}$ or above 19 m/sec.

Other Complications. In addition to the gust-scale, instrumental, advective, and non-steady state wind variations, two other complications arise in the planetary boundary layer to prevent the observation of the

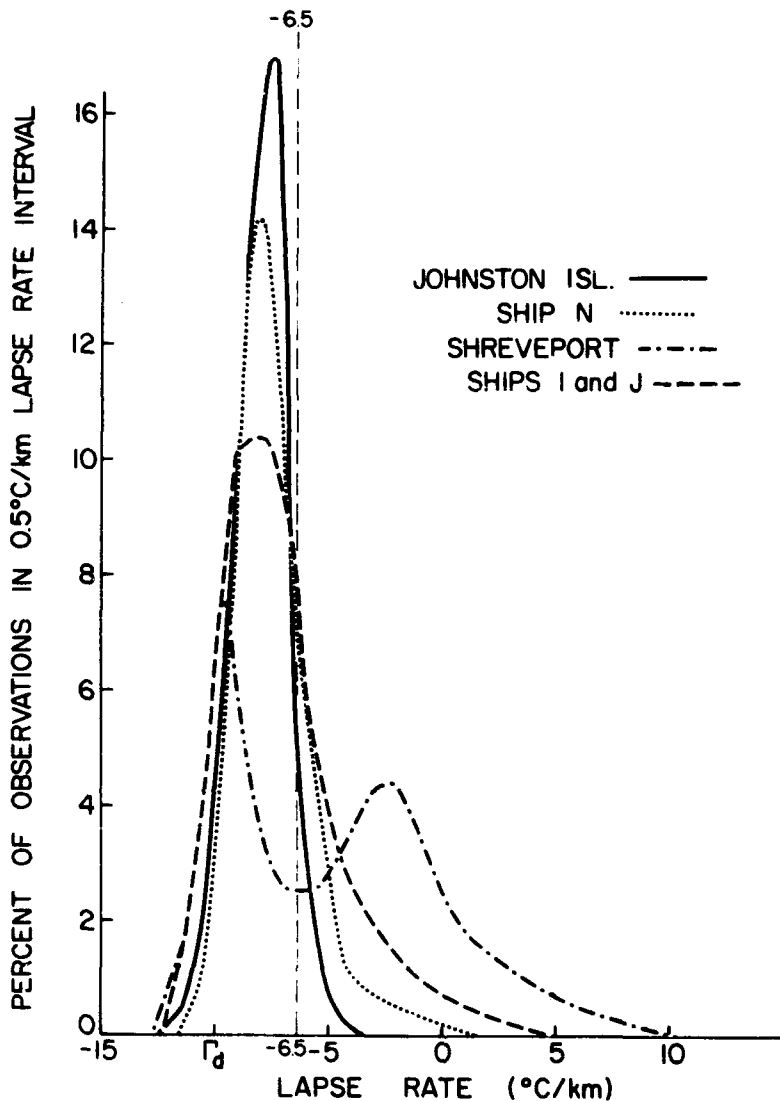


Fig. 9. Normalized frequency distributions of lapse rate in surface 900 mb layer (from Mendenhall, 1967).

simple Ekman profile. These are:

1. Vertical stability variations
2. Horizontal temperature gradient variations (thermal wind or geostrophic veering influence)

Stability Variations. Stability influences are a major factor in the veering character over land. Over the oceans, diurnal stability varia-

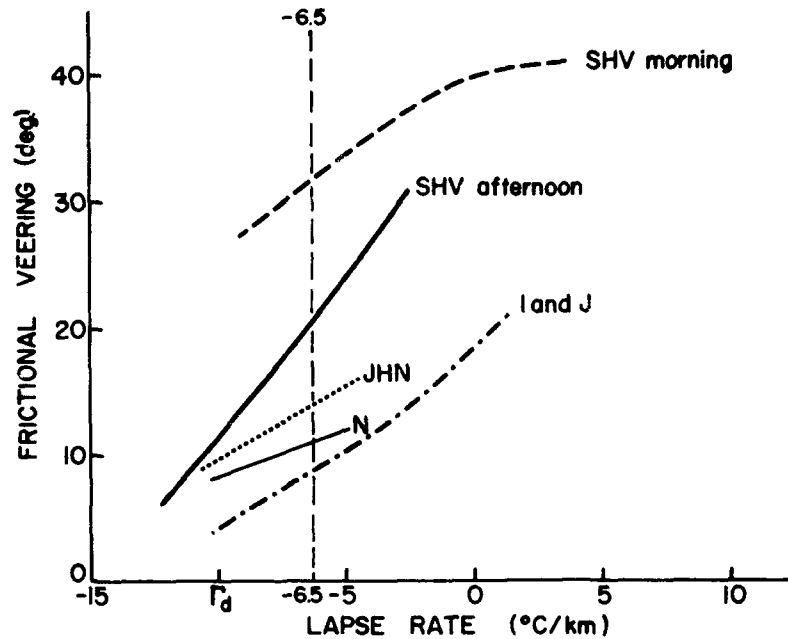


Fig. 10. Frictional veering (with geostrophic veering effect accounted for and removed) as a function of lapse rate in the surface to 900 mb layer at each station. Smooth lines were obtained by averaging frictional veering in classes of lapse rate and connecting the points (from Mendenhall, 1967).

tions are small and do not significantly influence the veering. Fig. 9 shows the much larger lapse rate variations at Shreveport (a typical land station) compared with lapse rate variations at weather ships I, J, N and Johnston Island. Fig. 10 shows the variations of frictional veering with lapse rate in the surface-to-900 mb layer for these same stations. Veering is directly related to stability. On the average the 1st km oceanic veering decreases about 10° for stability changes from isothermal to dry-adiabatic.

Stability variations over the oceans are typically small. The influence of p. b. l. oceanic lapse rate variations are thus not felt to be a dominant influence in determining differences in observed veering.

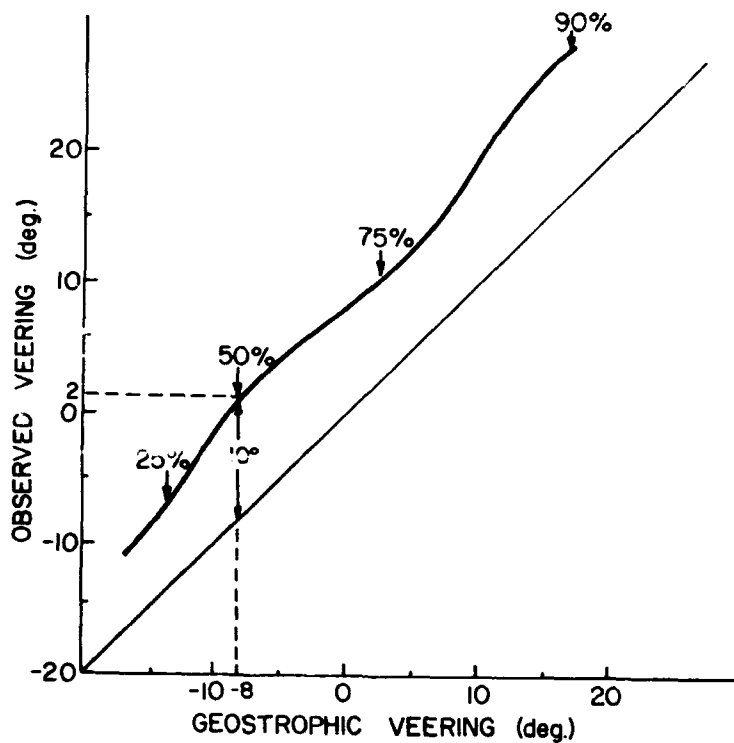


Fig. 11. Observed veering in the surface to 900 mb layer at Ship N as a function of geostrophic veering, obtained by averaging observed veering in 5° class intervals of geostrophic veering. The heavy line connects these average values. The dashed lines indicate that the median ("50%") geostrophic veering is -8° and that the median observed veering is 2° . The difference of 10° is the median frictional veering. The thin sloping line connects points of equal observed and geostrophic veering, or where frictional veering equals zero. The vertical distance between the lines thus represents frictional veering and is indicated by arrows at the median point. The "75%" mark indicates that 75% of the observations had geostrophic veering of less than 3° , etc. Sample size: 2386 observations (from Mendenhall, 1967).

Horizontal Temperature Gradient Variations. In contrast the thermal wind influence (or geostrophic veering) can be very pronounced with cold and warm air advection and must always be accounted for.* Thermal wind or geostrophic veering influences are felt to be largely elim-

* It is only the temperature gradient along the direction of motion which significantly alters the measured veering.

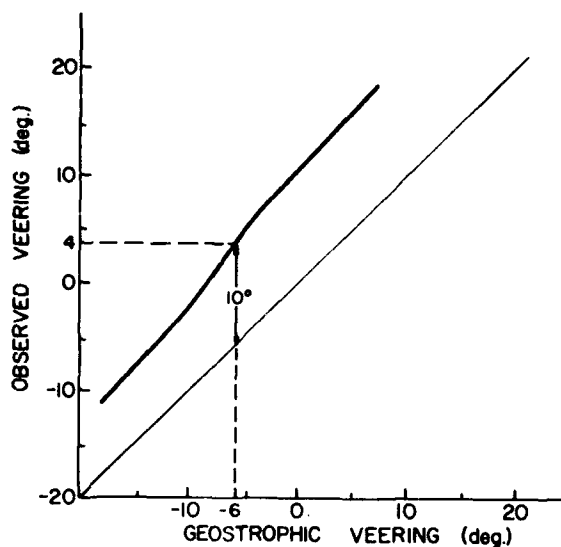


Fig. 12. Observed veering in the surface to 900 mb layer at Johnston Island as a function of geostrophic veering. (See Fig. 11 for further description). Dashed lines indicate median geostrophic veering of -6° and median observed veering of 4° . Difference of 10° is median frictional veering. Sample size: 3667 observations (from Mendenhall, 1967).

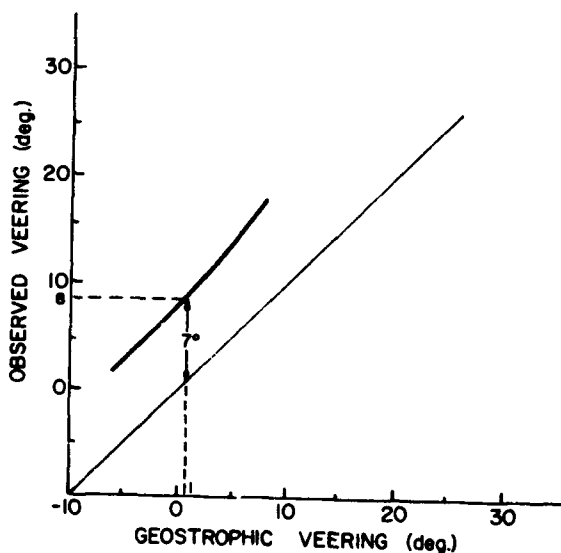


Fig. 13. Observed veering in the surface to 900 mb layer at Ships I and J as a function of geostrophic veering. (See Fig. 11 for further description). The median frictional veering of 7° is indicated by arrows. (Original data after Findlater et al., 1966; from Mendenhall, 1967).

inated by assuming constant baroclinicity** through the lowest two kilometers and then subtracting the veering of the second km being assumed to be a product of the thermal wind alone. If the observed wind veering in the first and second km layer is 15° and 5° , respectively, then the thermal wind influence would be assumed to be 5° . This 5° veering would be subtracted from the first km veering data and a frictional veering of 10° would be accepted. This procedure has been verified by measuring the 1st km horizontal temperature gradients directly and determining how this gradient compares with the one obtained by subtracting the second km veering. It has been found to be generally satisfactory but not representative at stations with an inversion layer below 800 mb.

The subtraction of the thermal wind influence can reduce and normalize the frictional veering as has been demonstrated by Mendenhall, 1967 (see Figs. 11-13). Fig. 11 shows the frequency distribution of observed veering as a function of geostrophic veering (or thermal wind) at weather ship N. Similar plots of observed vs. geostrophic veering are shown in Figs. 12 and 13 for Johnston Island and weather ships I and J (data from Findlater et al., 1966). Note how large the thermal wind correction can be. Note also, that after it is made, the average frictional veering is $\sim 10^{\circ}$.

The small net veering at Ship N in Fig. 1 is due to cold air advection. Warm air advection is occurring at Swan Island (Fig. 2). Subtrac-

**Thermal wind influence, geostrophic veering, baroclinicity are synonymously used.

tion of these opposite acting thermal wind influences largely reduces these veering differences.

Summary. Observed wind veering is a function of a number of simultaneously acting influences, Thus,

$$\begin{array}{rcccccc}
 \text{Observed} & = & \text{Frictional} & + & \text{Geostrophic} & + & \text{Stability} & + & \text{Unrepre-} & + & \text{Local and} \\
 \text{Veering} & & \text{Veering} & & \text{or Thermal} & & \text{Change} & & \text{sentative} & & \text{Advective} \\
 & & & & \text{Wind Veer-} & & \text{Veering} & & \text{Turbulent} & & \text{Veering} \\
 & & & & \text{ing} & & & & \text{and Instru-} & & \text{Change} \\
 & & & & & & & & \text{ment Veer-} & & \\
 & & & & & & & & \text{ing} & & \\
 A & = & B & + & C & + & D & + & E & + & F
 \end{array}$$

The attempt of this paper is to determine B from large statistical samples of A. E veering influences are eliminated by averaging over a large data sample. D and F veering influences are accounted for or eliminated by averaging over a large data sample, a long period, and a large longitude (360°) belt. C veering influences are eliminated or accounted for by large time and space averaging and by assuming constant baroclinicity with height and subtracting the 2nd km veering from the 1st km. This is shown to be very effective. Thus, B is determined from A after the veering influences of C, D, E, and F have been eliminated or accounted for and subtracted out.

III. DATA SAMPLE

Two primary oceanic upper air data sources are involved: islands and atolls, and ships.

Islands and Atolls Data. This data consists of regular island or atoll upper air reporting sites from which two or four daily soundings are available. This stationary group of observations has been analyzed in three groups.

- 1) fifteen of the stations were sampled continuously for a 6 month summer period in the early 1960's. Table 1 summarizes the information on these 15 stations obtained from the U.S. Weather Bureau Northern Hemisphere Data Tabulations.
- 2) veering information was extracted from tropical stations during 1967-69 in the Western Pacific and in the West Indies-Gulf of Mexico region. This data was obtained in connection with the large statistical studies of tropical cloud clusters (Williams, 1970) and clear areas which the author and his graduate students have been investigating. The data was stratified only by ocean and latitude (greater than or less than 18°). Wind information was obtained from magnetic tape images of card deck 645 of the National Climatic Center, Asheville, North Carolina, at the surface, 1000, 950, 900, 850 and 800 mb. Winds are reported to the nearest m/sec and in direction to the nearest degree.
- 3) a smaller portion of the 1967-69 data was separated into individual cloud cluster and clear area veering groups. Data source is the same as in 2). Figs. 14 and 15 show the locations of the stations used in the latter two data groups.

80,000 Ocean Ship Veering Reports from 1949-1964. Nearly all U.S. National Climatic Center, Asheville, North Carolina data on the variation of wind in the lowest two km over the oceans has been assembled for the 16-year period of 1949-64. Data includes over 80,000 ship rawin and pibal observations from merchant ships which took rawins or pibals, weather ships, military ships--every kind of surface vessel

Table 1
Geographical Data on Stationary Locations

<u>Name</u>	<u>Location</u>	<u>Months of Observations</u>	<u>Highest Point (meters)</u>	<u>Height (meters) and Location of Observing Station</u>
<u>Pacific</u>				
Marcus I.	24N, 154E	6	22	20, center part
Midway I.	28N, 177W	6	14	13, center
French Frigate Shoals	24N, 166W	6	70 (volcanic rock)	3
Johnston I.	16N, 170W	6	22	2, north side
Wake I.	20N, 166E	5	7	4, SE side
Eniwetok Atoll	11N, 162E	6	4	3, SE side
Kwajalein Atoll	9N, 168E	6	3	3, center
Majuro Atoll	7N, 171E	6	5	5, west side
Palmyra	5N, 162W	1½	3	2
Weather Ship V	34N, 164E	6	25	10
<u>Atlantic</u>				
Grand Turk I.	22N, 71W	6	10	5
Grand Cayman I.	19N, 81W	6	10	5
Swan I.	17N, 84W	6	10	5
San Andrés I.	12N, 82W	6	110	5
Weather Ship E	35N, 48W	10	25	10

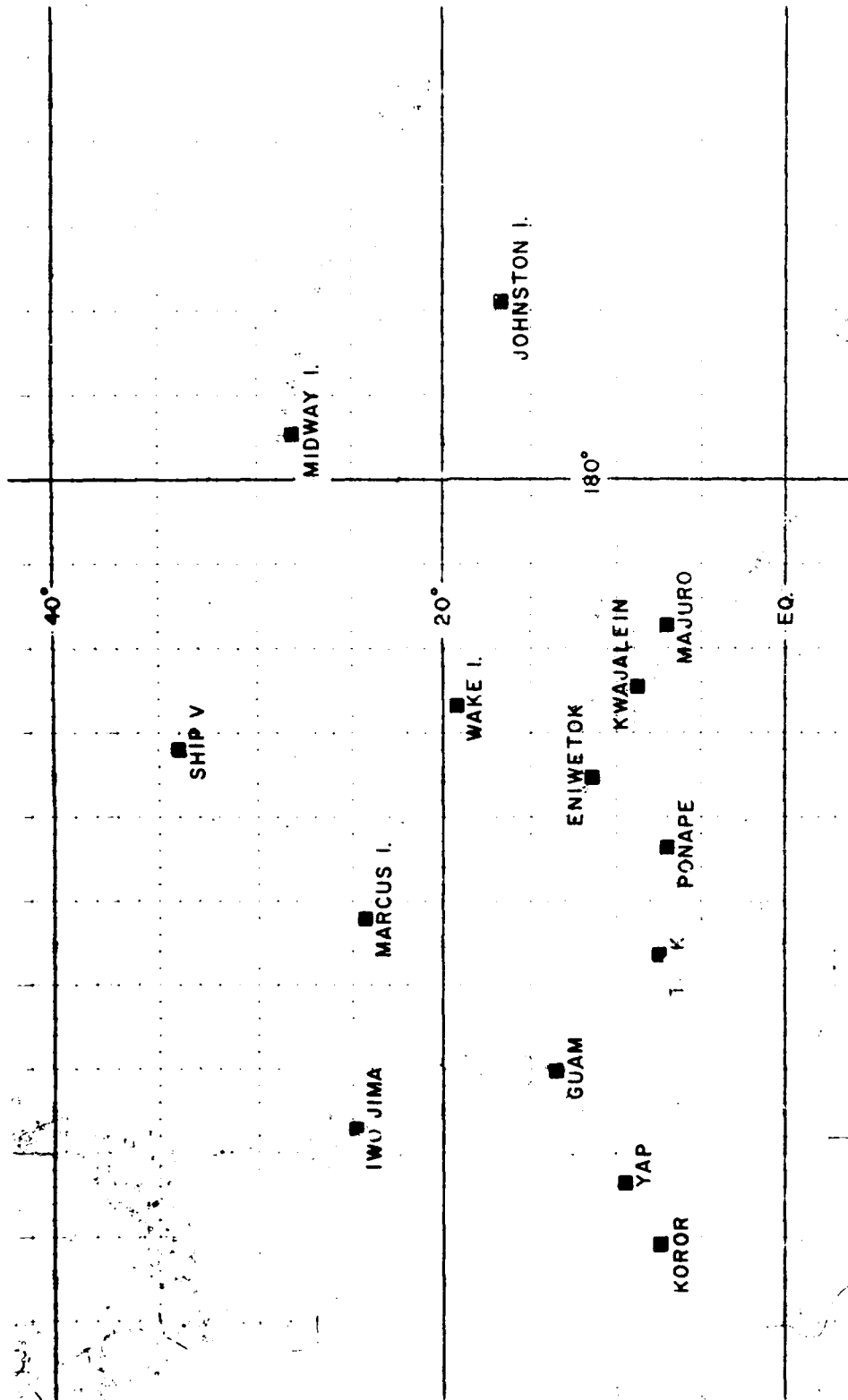


Fig. 14. Pacific upper air stations from which veering information of Tables 5 and 6 was obtained.

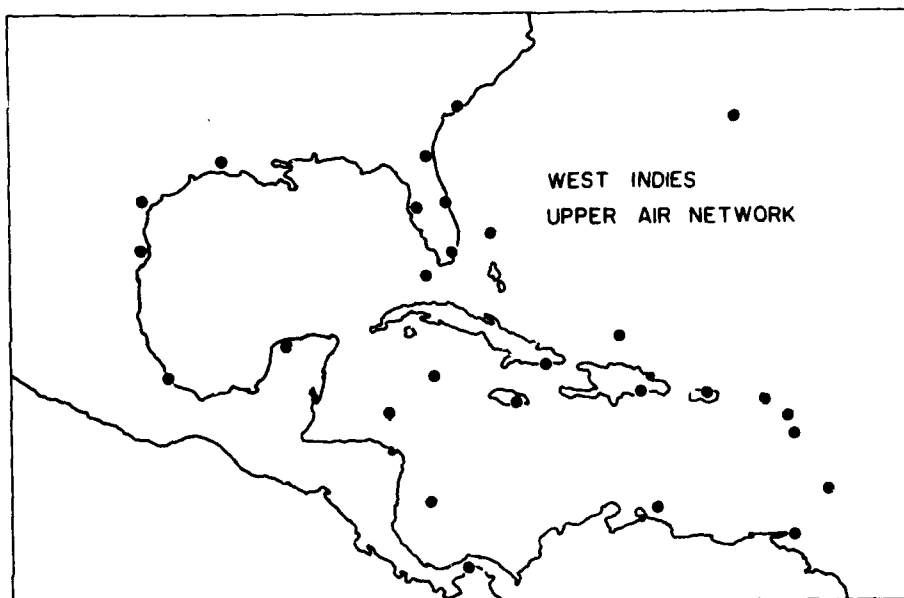


Fig. 15. Stations from which veering information in Tables 5 and 6 was obtained.

which Asheville had on record.

Between 1949 and 1955 (data set I) wind reports were available for the surface, 500 m, 1 km, 1.5 km and 2 km and directions were reported on the 16 point compass ($22\text{-}1/2^\circ$ intervals). A little less than half the data is in this category. The reports of the 1956 through 1964 period (data set II) give wind information to the nearest degree and by height at the surface, 150, 300, 500, 1 km, 1.5 km to 2 km. Veering was obtained from the earlier (1949-55) 16 point compass data by assuming the mean wind direction of each 16 point direction category and noting changes of category with height. In the statistical average this proved very satisfactory.

Data stratifications were performed on each of the two data sets separately. At all levels and in all stratifications, only very small data

set differences were found. To increase the sample size, the author felt quite justified in averaging both data samples together. This was accomplished by 500 m height intervals. Figs. 16-18 give the number of observations available in each 10° latitude-longitude area. These figures show how the two ship data sets and the combined data sample (sets I and II) are distributed geographically. Data is concentrated along the shipping routes, but a fairly good latitudinal and longitudinal distribution is present.

Some of the ship reports had to be eliminated because of missing information at some levels, or if speeds, shears, or veering angles were unrealistically excessive. After this screening analysis there were 60,000 ship reports remaining. Over 5000 observations are available in the latitude belt from 10° - 20° N. This ship information has been stratified by latitude, season, wind direction and wind speed. Component wind shears along and perpendicular to the wind at 2 km have been printed out by 500 m intervals. In addition, averaging was performed to obtain the wind speed squared and cubed. Vertical gradients of this information were taken at the various reporting levels. Fig. 19 shows a typical data printout of this ship vessel information for data set II. Symbols are defined in Table 2 and the stratifications which were made are shown in Table 3.

Since 1964 this class of ship data is available only at 50 mb intervals. This type of vertical resolution is no longer available.

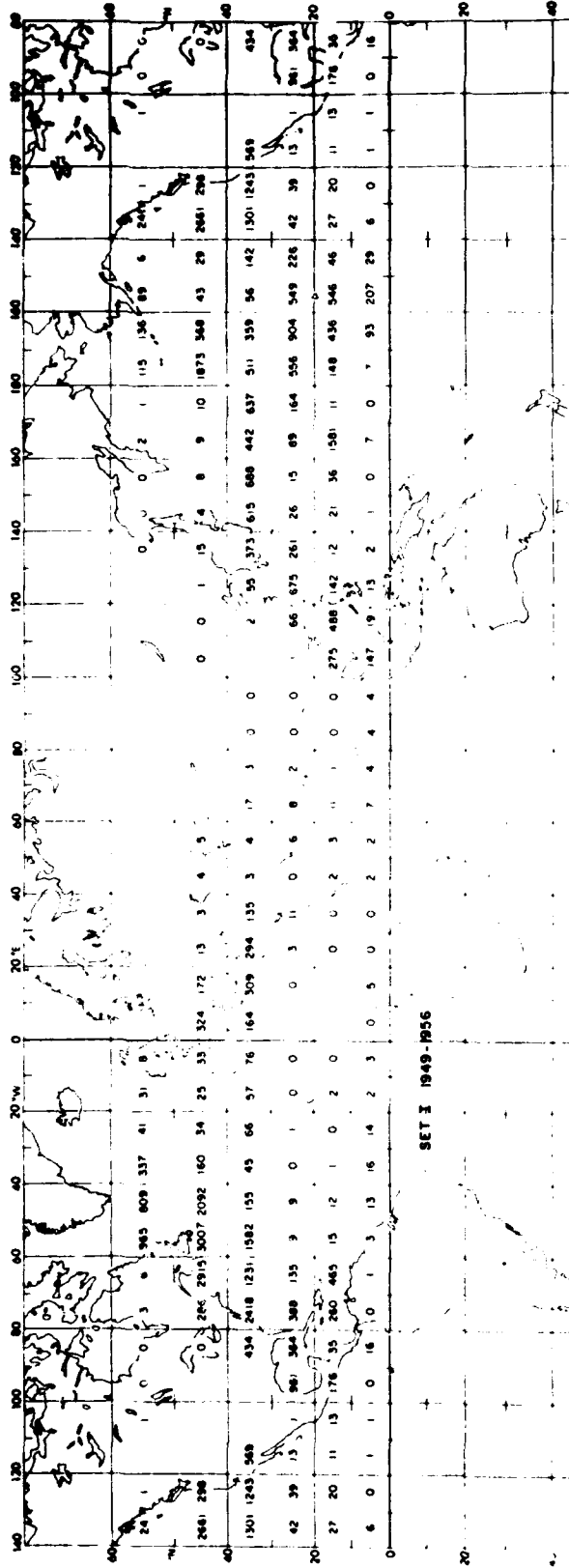


Fig. 16. Distribution of ship pibal and rawin data for period of 1949-1955.

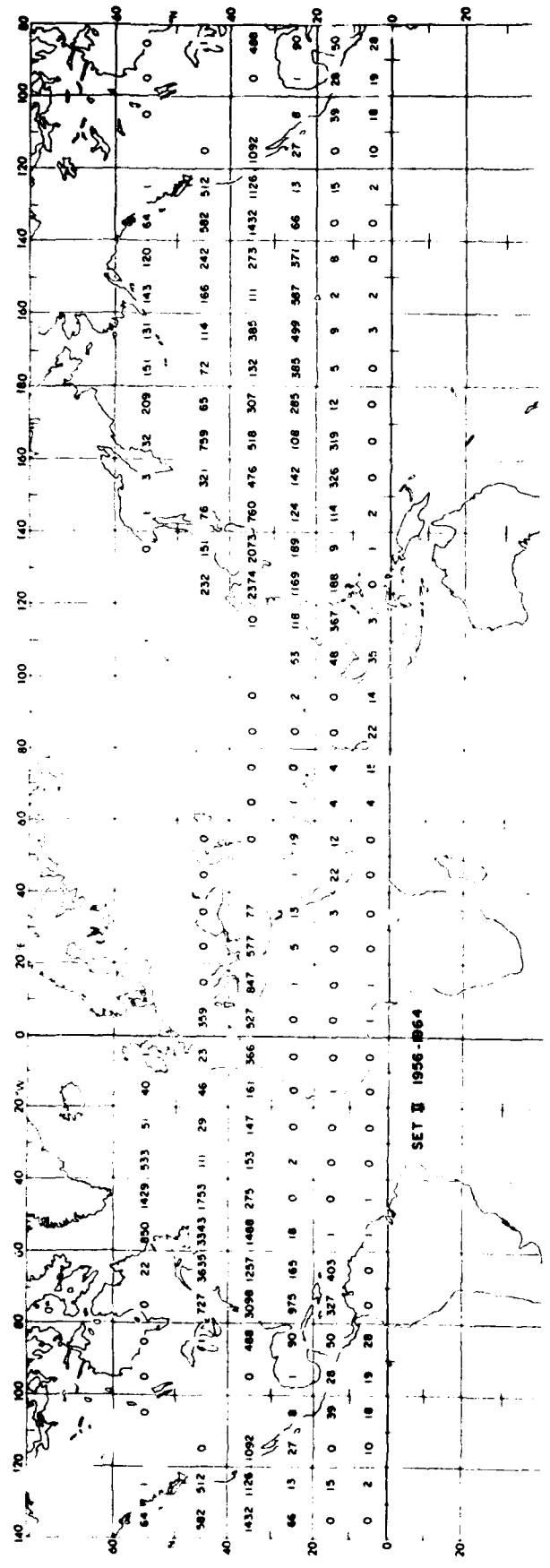


Fig. 17. Distribution of ship pibal and rawin data for period of 1956-1964.

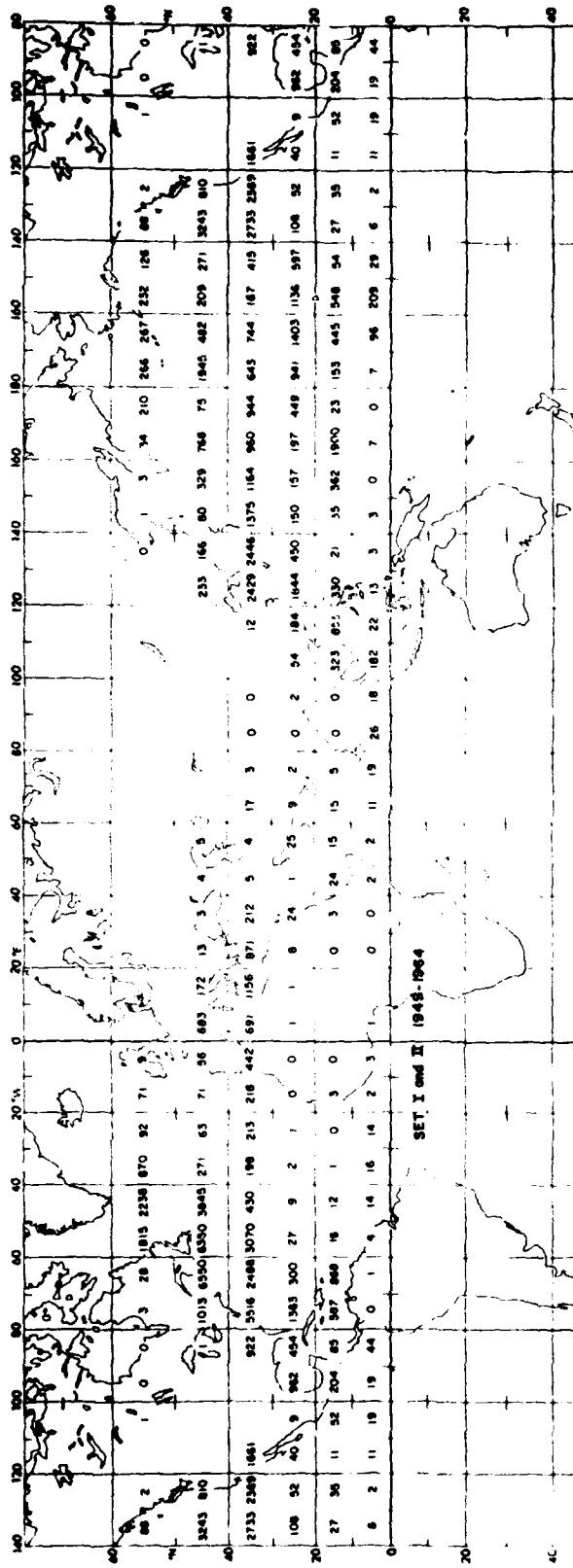


Fig. 18. Distribution of ship pibal and rawin data for combined period of 1949-1964.

Table 2

DEFINITION OF SYMBOLS

- (1) SB - The average value of the wind speed; $\frac{\Sigma V_i}{N}$; [Units-m/sec];
N = # of obs.; V = speed
- (2) S2 - The average value of the square of the wind speed;
 $\frac{\Sigma (V_i)^2}{N}$ [Units-m²/sec²]
- (3) S3 - The average value of the cube of the wind speed; $\frac{\Sigma (V_i)^3}{N}$
[Units-m³/sec³]
- (4) u - The component of the resultant vector wind along the x-axis
(in the meteorological coordinate system). $\frac{\Sigma u_i}{N}$ [Units-m/sec]
- (5) v - The component of the resultant vector wind along the y-axis
(in the meteorological coordinate system). $\frac{\Sigma v_i}{N}$
- (6) UA - The average shear (between the indicated levels) parallel to
the wind direction at the lower level. A positive UA
indicates the component of the wind along the direction
of flow at the lower level is increasing with height.
- (7) VA - The average shear (between the indicated levels) perpendicular
to the wind vector at the lower level. Here a positive
VA indicates the wind is veering with height.
- (8) VS - The average of the absolute values of the observed vertical
wind shear; $VS = \frac{\Sigma \sqrt{(UA)^2 + (VA)^2}}{N}$
- (9) DD - The wind veering computed from the values of VA and SB; generally
 $DD = \text{ATAN}\left(\frac{VA}{SB}\right) \times 57.3$ Here the value of SB at the
lower level was used.
- (10) DA - Mean wind veering computed using wind direction data and the
following limits:
(1) All calm winds were neglected.
(2) All cases with winds greater than 30 m/sec at any
level were neglected.
(3) All cases with direction changes greater than 45°
between two successive levels or greater than 90°
between any of the levels were neglected.
- (11) DR - Mean wind veering computed using wind direction data and the
following limits:
(1) All winds less than 3 m/sec were neglected.
(2) Other criteria are the same as those in (2) and (3) for DA.

ALL CASES

1956-1964

30 TO 40 DEGREES LATITUDE 1400H CASES

U²

U²

U²

U²

U²

U²

U²

U²

U²

U²

SFC
 150 U= 1.6 U= 1.9 U= 2.2 U= 2.5 U= 3.3 U= 4.3 U= 5.4
 VS= 1.4 VS= 1.9 VS= 2.2 VS= 2.5 VS= 3.3 VS= 4.3 VS= 5.4
 300 U= 1.7 U= 2.0 U= 2.3 U= 2.6 U= 3.0 U= 3.5 U= 4.0
 VS= 1.5 VS= 1.8 VS= 2.1 VS= 2.4 VS= 2.8 VS= 3.2 VS= 3.6
 500 U= 1.8 U= 2.1 U= 2.4 U= 2.7 U= 3.1 U= 3.5 U= 4.0
 VS= 1.6 VS= 1.9 VS= 2.2 VS= 2.5 VS= 2.9 VS= 3.3 VS= 3.7
 1000 U= 1.9 U= 2.2 U= 2.5 U= 2.8 U= 3.2 U= 3.6 U= 4.0
 VS= 1.7 VS= 2.0 VS= 2.3 VS= 2.6 VS= 3.0 VS= 3.4 VS= 3.8
 1500 U= 2.0 U= 2.3 U= 2.6 U= 2.9 U= 3.3 U= 3.7 U= 4.1
 VS= 1.8 VS= 2.1 VS= 2.4 VS= 2.7 VS= 3.1 VS= 3.5 VS= 3.9
 2000 U= 2.1 U= 2.4 U= 2.7 U= 3.0 U= 3.4 U= 3.8 U= 4.2
 VS= 1.9 VS= 2.2 VS= 2.5 VS= 2.8 VS= 3.2 VS= 3.6 VS= 4.0

4537 CASES

150-SFC 300-150 500-300 1000-500 1500-1000 2000-1500 500-SFC 1000-SFC 2000-1000 (1000-SFC)
 UA= .1 UA= .2 UA= .3 UA= .4 UA= .5 UA= .6 UA= .7 UA= .8 UA= .9
 VA= .3 VA= .4 VA= .5 VA= .6 VA= .7 VA= .8 VA= .9 VA= 1.0 VA= 1.1
 VS= 1.0 VS= 1.1 VS= 1.2 VS= 1.3 VS= 1.4 VS= 1.5 VS= 1.6 VS= 1.7 VS= 1.8
 VD= 1.0 VD= 1.1 VD= 1.2 VD= 1.3 VD= 1.4 VD= 1.5 VD= 1.6 VD= 1.7 VD= 1.8
 DA= 1.0 DA= 1.1 DA= 1.2 DA= 1.3 DA= 1.4 DA= 1.5 DA= 1.6 DA= 1.7 DA= 1.8
 DR= 1.0 DR= 1.1 DR= 1.2 DR= 1.3 DR= 1.4 DR= 1.5 DR= 1.6 DR= 1.7 DR= 1.8
 UA= .1 UA= .2 UA= .3 UA= .4 UA= .5 UA= .6 UA= .7 UA= .8 UA= .9
 VA= .3 VA= .4 VA= .5 VA= .6 VA= .7 VA= .8 VA= .9 VA= 1.0 VA= 1.1
 VS= 1.0 VS= 1.1 VS= 1.2 VS= 1.3 VS= 1.4 VS= 1.5 VS= 1.6 VS= 1.7 VS= 1.8
 VD= 1.0 VD= 1.1 VD= 1.2 VD= 1.3 VD= 1.4 VD= 1.5 VD= 1.6 VD= 1.7 VD= 1.8
 DA= 1.0 DA= 1.1 DA= 1.2 DA= 1.3 DA= 1.4 DA= 1.5 DA= 1.6 DA= 1.7 DA= 1.8
 DR= 1.0 DR= 1.1 DR= 1.2 DR= 1.3 DR= 1.4 DR= 1.5 DR= 1.6 DR= 1.7 DR= 1.8

150-SFC 300-150 500-300 1000-500 1500-1000 2000-1500 500-SFC 1000-SFC 2000-1000 (1000-SFC)
 UA= .1 UA= .2 UA= .3 UA= .4 UA= .5 UA= .6 UA= .7 UA= .8 UA= .9
 VA= .3 VA= .4 VA= .5 VA= .6 VA= .7 VA= .8 VA= .9 VA= 1.0 VA= 1.1
 VS= 1.0 VS= 1.1 VS= 1.2 VS= 1.3 VS= 1.4 VS= 1.5 VS= 1.6 VS= 1.7 VS= 1.8
 VD= 1.0 VD= 1.1 VD= 1.2 VD= 1.3 VD= 1.4 VD= 1.5 VD= 1.6 VD= 1.7 VD= 1.8
 DA= 1.0 DA= 1.1 DA= 1.2 DA= 1.3 DA= 1.4 DA= 1.5 DA= 1.6 DA= 1.7 DA= 1.8
 DR= 1.0 DR= 1.1 DR= 1.2 DR= 1.3 DR= 1.4 DR= 1.5 DR= 1.6 DR= 1.7 DR= 1.8

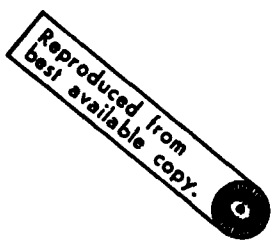


Fig. 19. Typical data printout by 10° latitude width of information for period 1956-1964. Symbols defined in Table 2.

Preceding page blank

Table 3

STRATIFICATIONS

1. ALL WINDS BY LATITUDE
2. NORTH WINDS BY LATITUDE
3. EAST WINDS BY LATITUDE
4. SOUTH WINDS BY LATITUDE
5. WEST WINDS BY LATITUDE
6. WINTER WINDS BY LATITUDE
7. SPRING WINDS BY LATITUDE
8. SUMMER WINDS BY LATITUDE
9. FALL WINDS BY LATITUDE
10. < 9 m/sec WINDS BY LATITUDE
11. > 9 m/sec WINDS BY LATITUDE
12. 0-4 m/sec WINDS BY LATITUDE
13. 5-7 m/sec WINDS BY LATITUDE
14. 8-11 m/sec WINDS BY LATITUDE
15. > 12 m/sec WINDS BY LATITUDE

Wind direction classification (based on direction at 500m level):

Set I.	N - (16, 1, 2)	Set II.	N - 316° - 45°	
1949-55	E - (4, 5, 6)	1956-64	E - 46° - 135°	points of compass classification
	S - (8, 9, 10)		S - 136° - 225°	
	W - (12, 13, 14)		W - 226° - 315°	

Season classification:

Winter -- January, February, March

Spring -- April, May, June

Summer -- July, August, September

Fall -- October, November, December

IV. WIND VEERING AT ISLANDS AND ATOLLS

Individual Station Long Term Veering. Table 4 lists the long term (mostly summer months except for the one and half month average at Palmyra during the Line Island Experiment) wind veering in the 1st and 2nd km layers for 15 individual island and atoll stations in the tropics and subtropics as described in Table 1. Observations were taken every 6 or 12 hours. More than 350 observations are available for most stations. Figs. 20 and 21 show the 6 month average vertical profiles of the variation of angle veering and wind speed through the lowest 2 km layers. Note the substantial differences between the 1st km veering (12° average) and the 2nd km veering (1° average). If the frictional veering is assumed to be approximated by the difference between the 1st and 2nd km layer veering, then a frictional veering of about 11° results. The assumption of constant thermal wind and the subtracting of the 2nd km veering from the 1st helps to reduce the 1 km veering spread. This is particularly so with the individual monthly veering values.

Individual Station Mean Monthly Veering. Figs. 22-29 portray the individual monthly average angle veerings for 8 of these 15 stations. Note how the individual monthly veerings can be significantly different from their 6 month averages. Difference in monthly thermal wind (as sea-surface temperature gradients change) are felt to be primarily responsible for these monthly veering differences. Lapse rate variations may also occur, but are believed to be only a secondary cause for these differences. It can be seen that subtraction of the monthly average 2nd

Table 4
 Veering Data at Stationary Locations
 Average Veering (degrees)

Name	Months of <u>Observations</u> (2 or 4 obs. per day)	(1 km-sfc)	(2 km-1 km)	(1 km-sfc)- (2 km-1 km)
<u>Pacific</u>				
Marcus I.	6	11	0	11
Midway I.	6	16	-2	18
French Frigate Shoals	6	3	-4	7
Johnston I.	6	5	-2	7
Wake I.	5	13	0	13
Eniwetok Atoll	6	4	-1	5
Kwajalein Atoll	6	12	1	11
Majuro Atoll	6	12	2	10
Weather Ship V	6	15	2	13
Palmyra	1½	9	0	9
<u>Atlantic</u>				
Grand Turk I.	6	17	2	15
Grand Cayman I.	6	15	3	12
Swan I.	6	21	2	19
San Andrés I.	6	12	4	8
Weather Ship E	10	<u>9</u>	<u>1</u>	<u>8</u>
<u>Average</u>		12	1	11

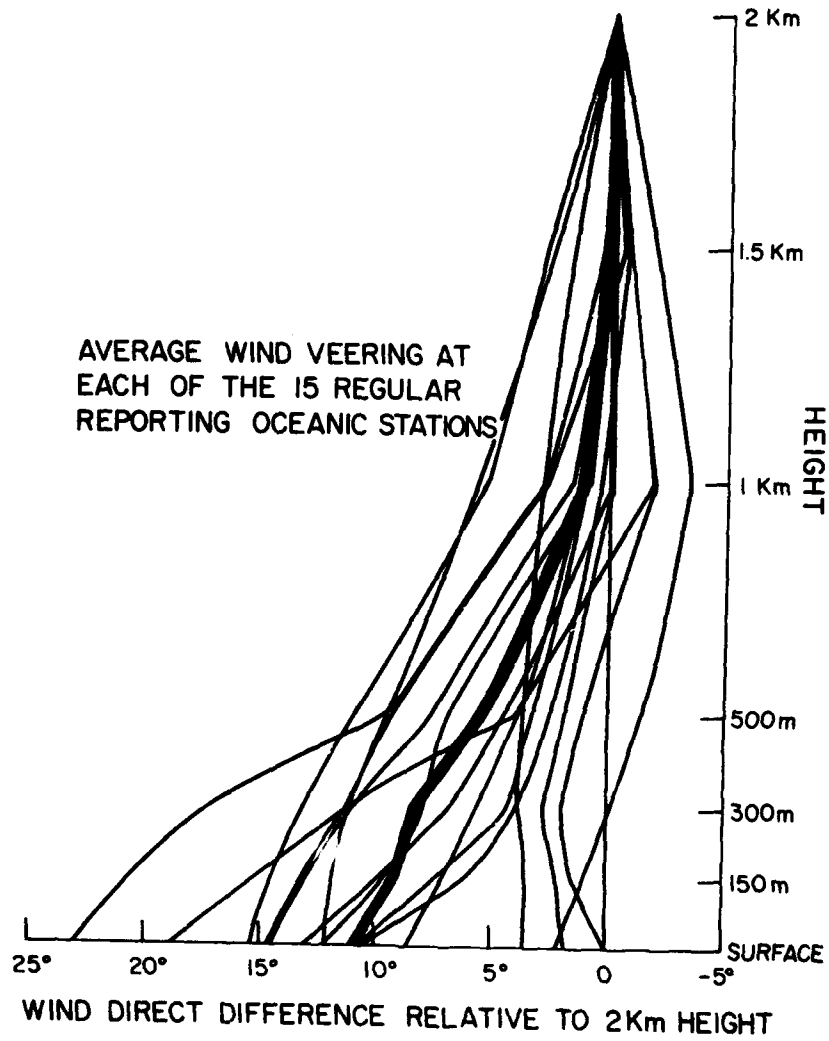


Fig. 20. Six month average of individual station wind veering.
Solid line represents the average of the 15 stations.

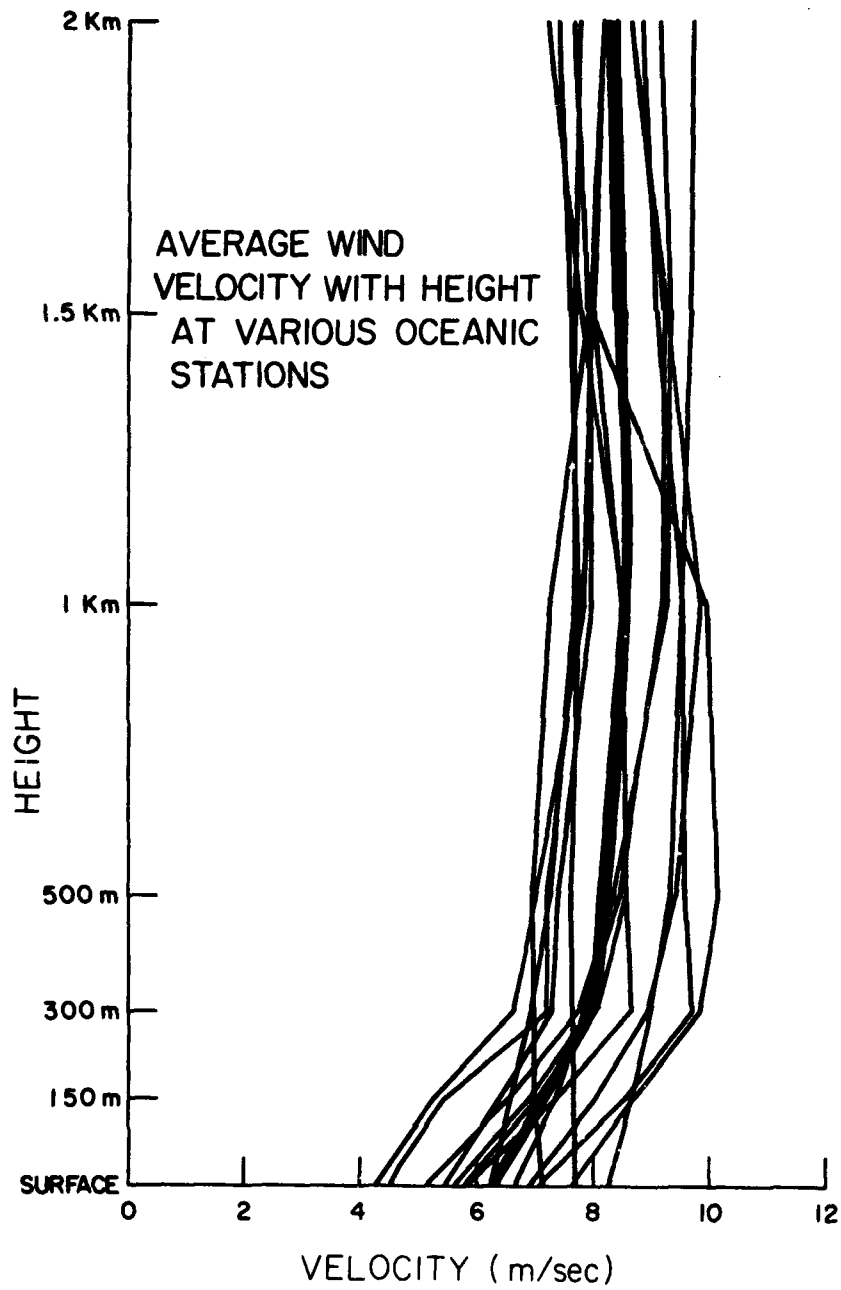


Fig. 21. Six month average of individual station tangential wind. Solid line represents the average of the 15 stations.

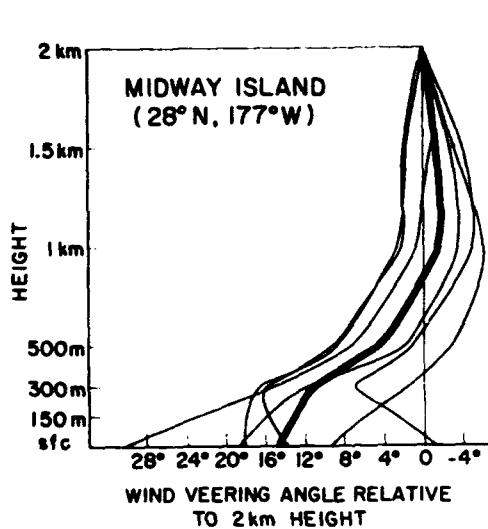


Fig. 22.

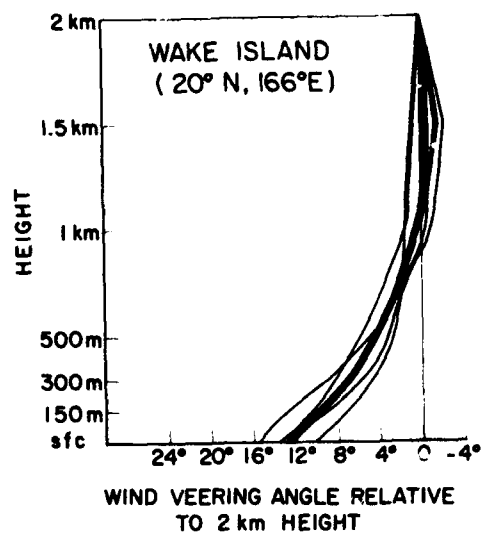


Fig. 23.

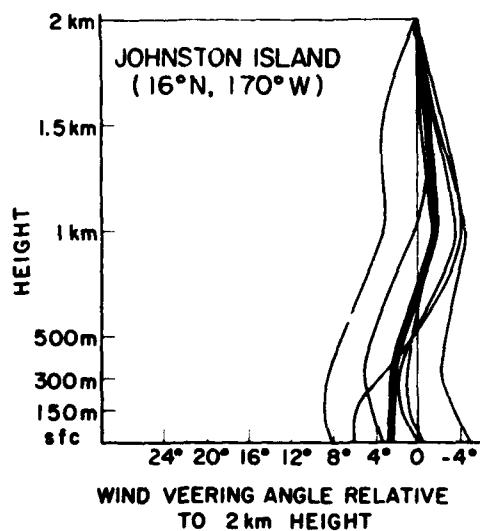


Fig. 24.

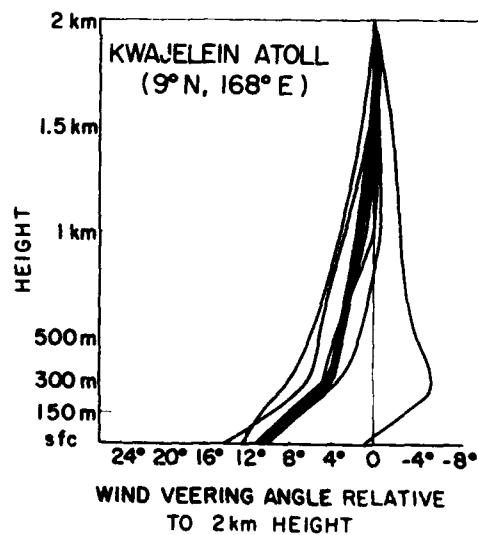


Fig. 25.

Figs. 22-25. Individual monthly mean wind direction variations in lowest two km layer and 6 monthly average (solid line).

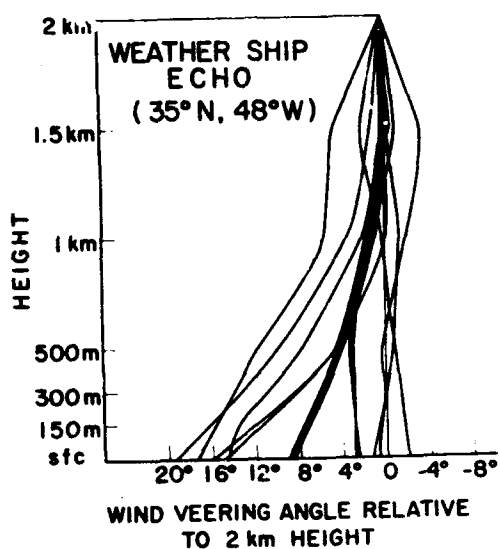


Fig. 26.

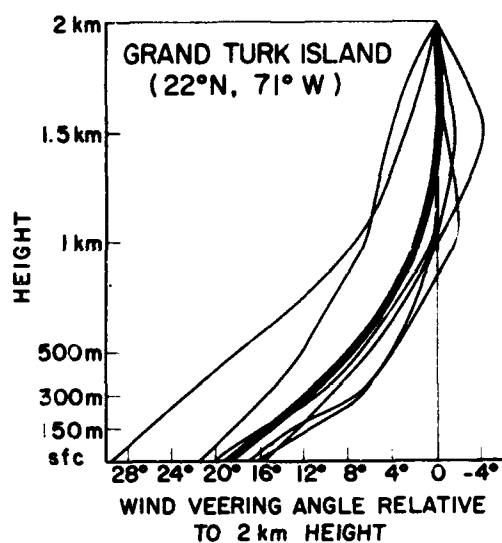


Fig. 27.

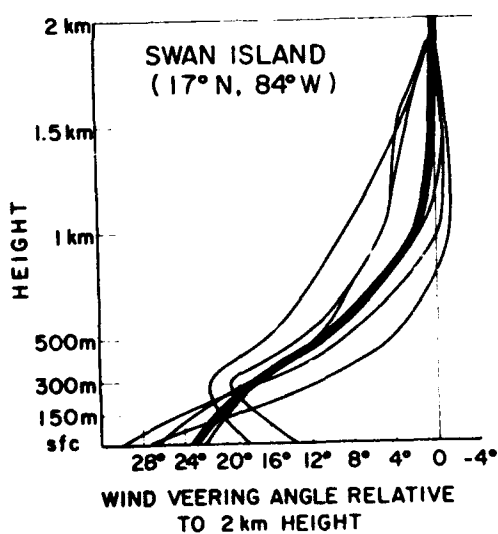


Fig. 28.

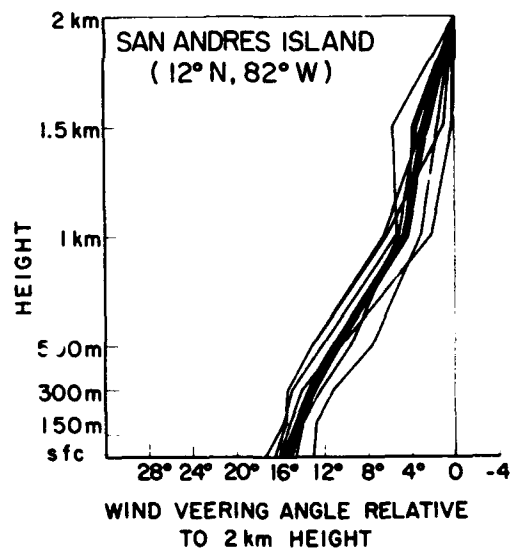


Fig. 29.

Figs. 26-29. Individual monthly mean wind direction variations in lowest two km layer and 6 monthly average (solid line).

km veering from the 1st km veering does help to reduce the spread of the profiles.

Veering Information from West Pacific and West Indies. This data was obtained in connection with the author's tropical cloud cluster and clear area studies from stations shown in Figs. 14 and 15. The data is not continuous and the stations have been mixed. Roughly equal amounts of data are available from all stations. Table 5 lists the 1st and 2nd km mean veering information for these two regions. The West Indies data has been divided into two latitude belts (greater and less than 18°). It is again to be noted that the 1st and 2nd km veerings average about 12° and 2° . The West Indies data north of 18° shows larger veerings.

Fig. 30 is the typical vertical profile of the veering from West Pacific atolls and selective surface ships surrounding the atolls. This figure shows that there is essentially no difference between the statistical averages of the island-atoll and the ship veering.

Cloud Cluster vs. Clear Area Veering. Table 6 shows the 1st and 2nd km wind veering for stations within 2° latitude of the center of satellite-observed tropical cloud clusters, and the same veering information relative to tropical clear regions. Note that for the clusters the 1st km veering is more (15° vs. 11°), but it extends well into the second km level, (6° veering for the clusters vs. 2° veering for the clear areas). This is to be expected if the cumulus clouds act to carry the turbulent sub-cloud layer momentum to higher levels. The clear area veering is very similar to the average of the ship and atoll-island stations. When

Table 5

	<u>1 km-sfc</u>	<u>2 km-1 km</u>	<u>(1 km-sfc) - (2 km-1 km)</u>
Western Pacific 7210 cases	10°	2°	8°
West Indies (less 18° latitude) 9205 cases	10°	3°	7°
West Indies (greater 18° latitude) 7980 cases	14°	3°	11°
AVERAGE	11°	3°	8°

Table 6

CLOUD CLUSTER vs. CLEAR AREA 1st and 2nd km VEERING

	<u>CLUSTERS</u>		
	<u>(1 km-sfc)</u>	<u>(2 km-1 km)</u>	<u>(1 km-sfc) - (2 km-1 km)</u>
Western Pacific (536 cases)	10°	4°	6°
West Indies (less 18° latitude) (266 cases)	13°	6°	7°
West Indies (greater 18° latitude) (244 cases)	27°	9°	18°
CLUSTER AVERAGE	15°	6°	9°
CLEAR AREAS AVERAGE	11°	2°	9°

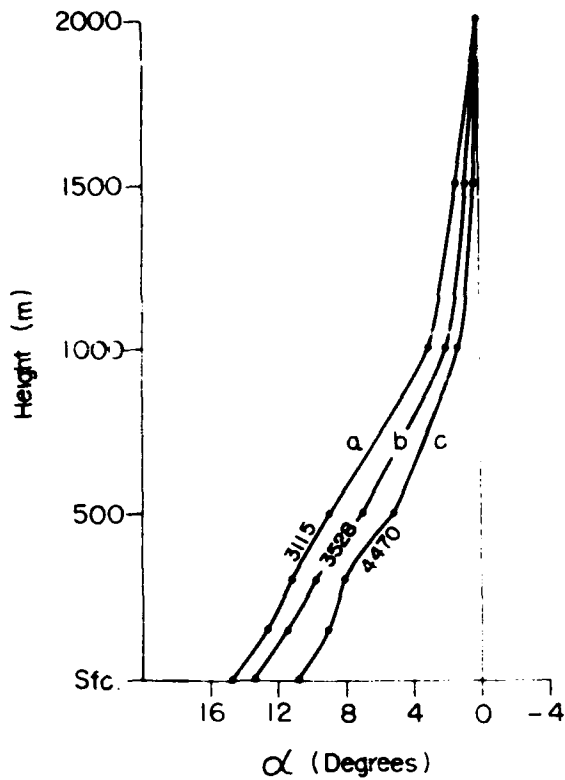


Fig. 30.

Observed wind angle veering with height in the lowest two km for atoll and ship reports of the tropical Pacific. Wind direction at two km is used as reference. Curve a represents veering of wind with height from ships which were located at least 1° latitude from any land. Curve b represents the frictional veering of wind with height as observed from atoll data; curve c as observed from ships located within 1° latitude of land. Number of observations in each class is shown on the figures.

the 2nd km veering is subtracted from the 1st km veering an equal 9° veering is observed for both the clusters and the clear areas.

Conclusion - The long term average from the tropical and sub-tropical islands and atolls indicate a typical 1st km 'frictional veering' as here defined of about 10° .

V. ANGLE VEERING FROM OCEAN SHIPS

Veering vs. Latitude. Figs. 31 and 32 portray the latitude distribution of the observed wind angle veerings for the lowest two km layers for data sets I (1949-55) and II (1956-64). There appears to be no significant latitude difference in the veerings of either data sample. The 1st km layer shows a distinct 10° greater veering than the 2nd km layer. Figs. 33 and 34 show the latitude distribution of the surface (10 m ship level) and 1 km wind components perpendicular to the two km wind. Positive values indicate veering. The one and two km winds have very small perpendicular component difference. The surface component perpendicular to the 2 km wind averages about 1 m/sec. The p.b.l. "frictional veering" due to mechanically disturbed gust-scale motions is now defined as the difference between the 1st and 2nd km layer veering angles as given in Figs. 31-32. This veering is also proportional to the perpendicular components as seen by the hatched area in Figs. 33 and 34.

Observing that there is very little difference in the data samples (as previously mentioned) the data of both samples were combined. Fig. 35 shows angle veering by 500 m layers from the 2 km reference level down to the surface. The small difference in veering angle variations with latitude and the much larger 1st km layer veering are clearly seen. Fig. 36 graphically portrays the entire oceanic Hemisphere average of the 1st and 2nd km layer veering angle differences. These average

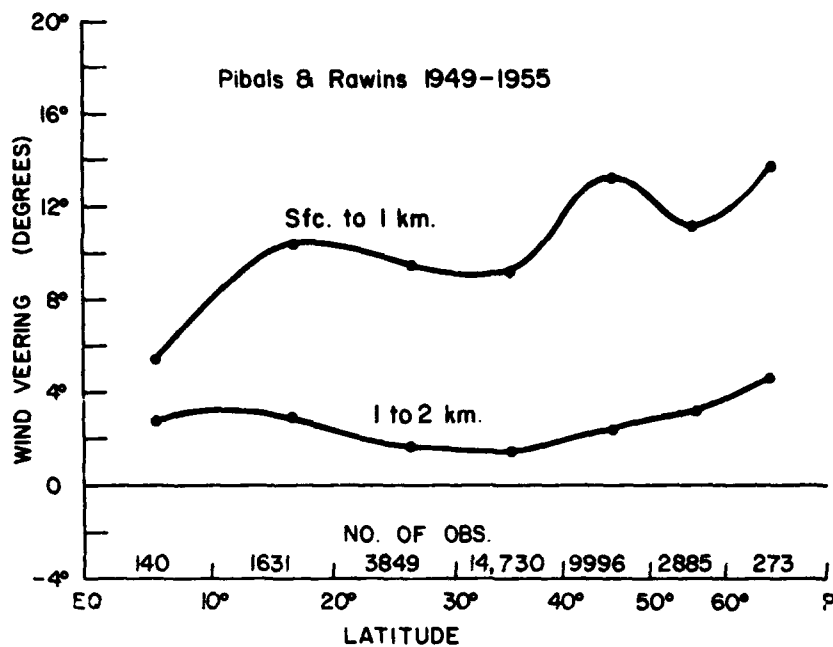


Fig. 31. Latitude variation of the average rawin and pibal ship wind veering in first and second km layer for 1949-1955 data where wind direction was reported to the 16 point compass.

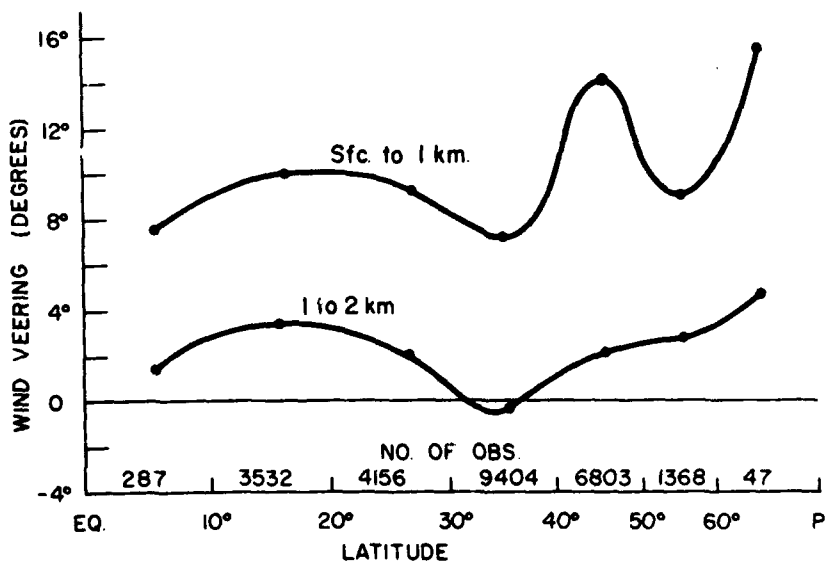


Fig. 32. Latitude variation of the average rawin and pibal ship wind veering in the first and second km layer for data of 1956-1964 where wind direction was reported to the nearest degree.

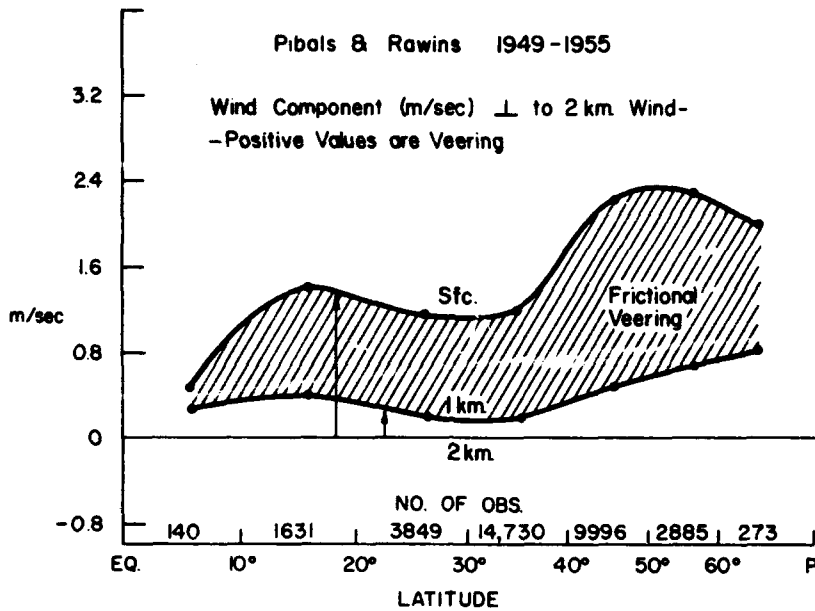


Fig. 33. Latitude distribution of surface (sfc) and 1 km wind components (m/sec) perpendicular to the second km wind for ship vessel data of 1949-1955. Hatched area portrays the assumed frictional veering which is the difference in surface and 1 km components.

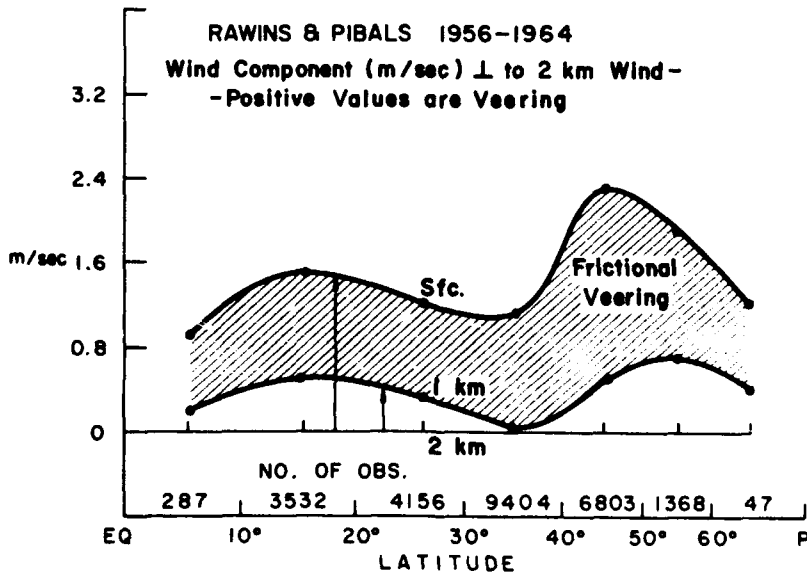


Fig. 34. Latitude distribution of surface (sfc) and 1 km wind component (m/sec) perpendicular to the second km wind for ship vessel data of 1956-1964. Hatched area portrays the assumed frictional veering which is the difference in the surface and 1 km components.

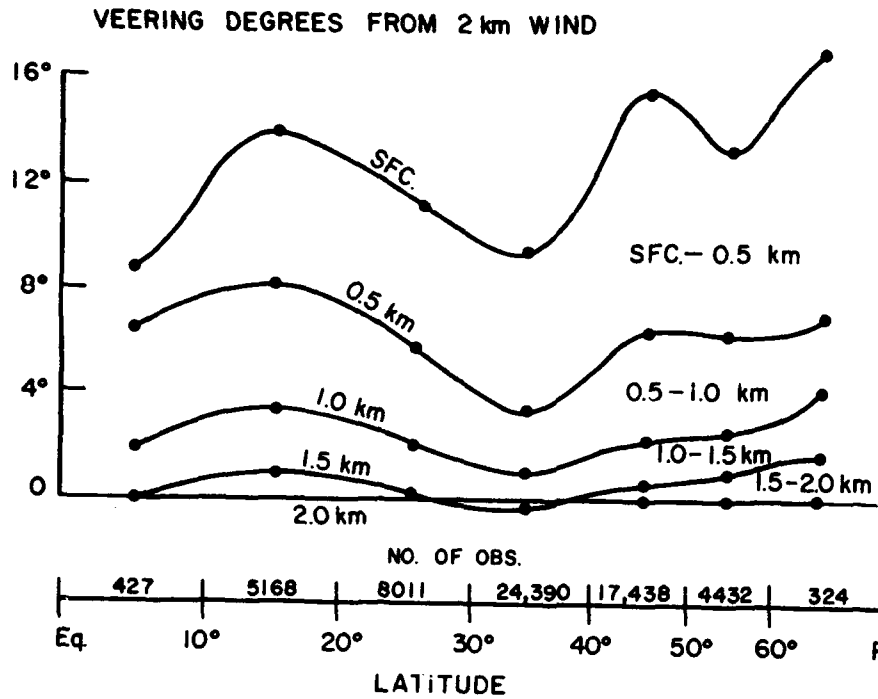
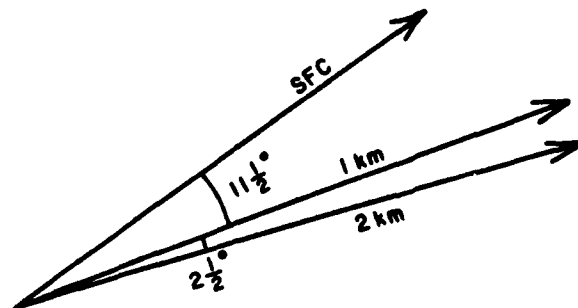


Fig. 35. Latitude distribution of wind direction veering in 500 m layers relative to the 2 km level wind for the entire data sample of 1949-1964.



**WIND VEERING IN FIRST
AND SECOND KM LAYER**

Fig. 36. Average of first and second km wind veering for all ship vessel data.

$\sim 11-1/2^\circ$ and $\sim 2-1/2^\circ$ giving a mean oceanic frictional veering in the 1st km layer of $\sim 9^\circ$.

Veering vs. Wind Direction and Latitude. Fig. 37 portrays the large difference of 1st km wind veering when the reports are stratified by wind direction to the four point compass as shown in Fig. 38. Note the 15° to 25° 1st km veering differences between north and south wind, yet east and west winds show only small veering differences. These north and south wind veering differences, believed to be due to thermal wind difference in cases of warm and cold air advection, are mostly eliminated when the 2nd km veering is subtracted from the 1st km wind with constant baroclinicity assumption. Fig. 39 shows both the 1st and 2nd km wind veering for north and south winds. When the 2nd km veering is subtracted from the 1st km veering the now defined 'frictional veering' is the same for both directions. The 20° and 10° average 1st and 2nd km veerings with south winds give a similar frictional veering as the 0° and -10° 1st and 2nd km veerings with north winds. Table 7 portrays this veering information in 20° latitude segments.

It is thus seen that there is no observed major 1st km 'frictional veering' difference with wind direction or latitude.

Veering vs. Wind Speed and Latitude. Figs. 40-43 show the 1st and 2nd km veering difference (ie. frictional veering) by latitude for wind speed categories of 0-4, 5-7, 8-11 and greater than 12 m/sec. It is observed that there are no primary 'frictional veering' differences associated with the four speed categories at all latitudes. Fig. 44 shows

COMBINED RAWIN AND PIBAL OBS.
OBSERVED WIND VEERING (DEGREES) IN Sfc. -1Km
LAYER BY WIND DIRECTION AND LATITUDE

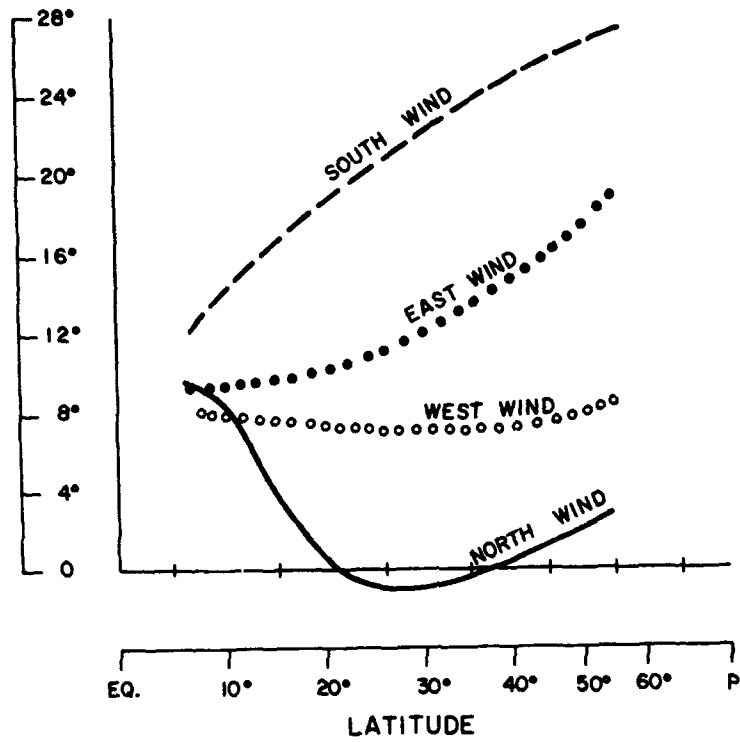


Fig. 37.

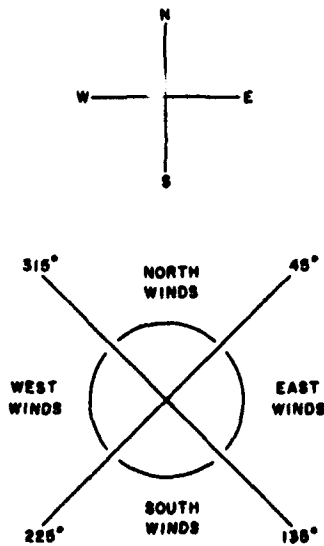


Fig. 38. Wind direction stratification.

NORTH AND SOUTH WIND VEERINGS (Degrees)
 1ST AND 2ND Km LAYERS AND DIFFERENCE —
 assumed to be the frictional veering.

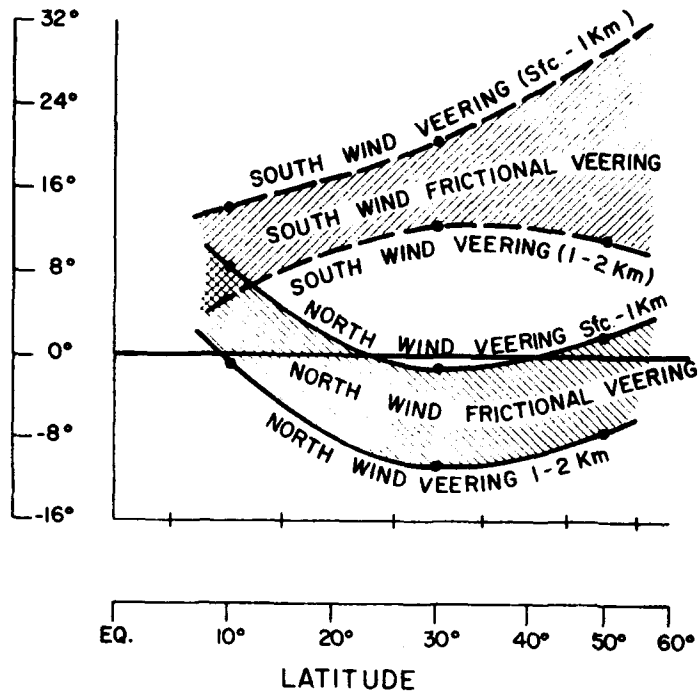


Fig. 39. Portrayal of 1st and 2nd km wind veering differences for north and south winds.

that there is no frictional veering difference with wind speed in the tropics and subtropics. In the westerly latitudes, however, strong winds show a frictional veering about twice that of the weak winds. The magnitude of the 2nd km veering is larger for higher wind speeds as was expected (See Discussion Section). Table 8 more explicitly shows this veering stratification by wind speed.

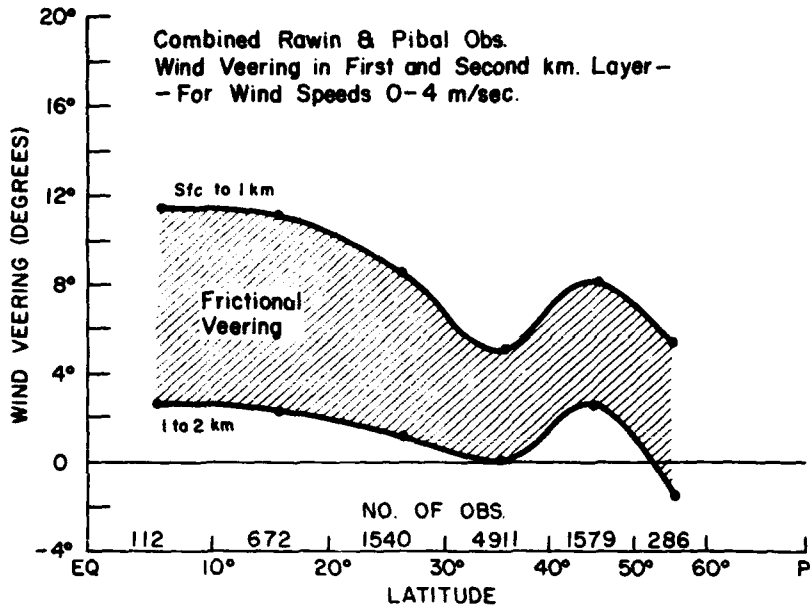


Fig. 40. Latitude distribution of frictional veering (hatched area) for 500 m winds of 0-4 m/sec.

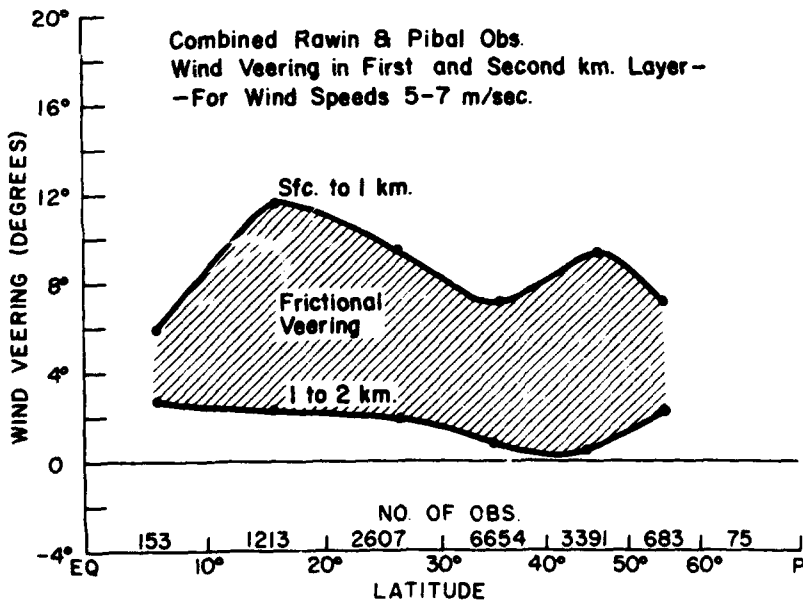


Fig. 41. Latitude distribution of frictional veering (hatched area) for 500 m winds of 5-7 m/sec.

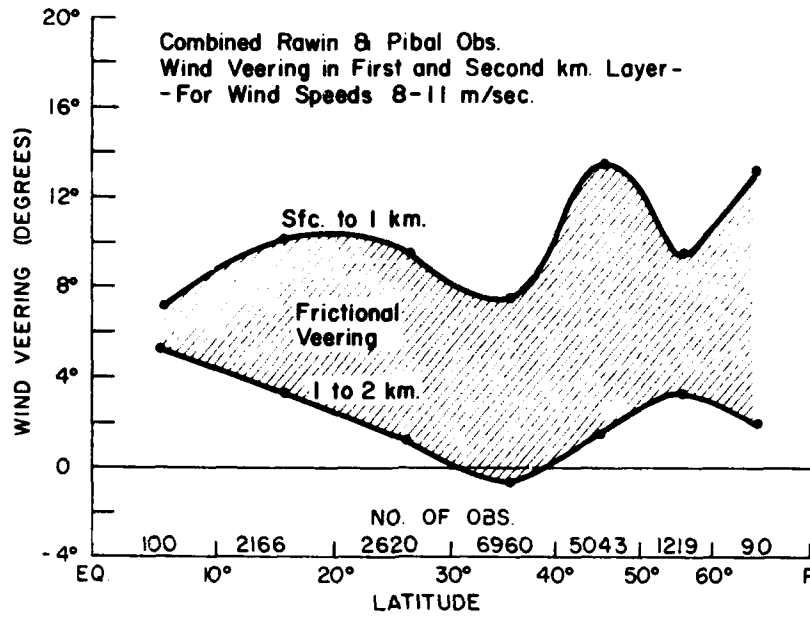


Fig. 42. Latitude distribution of frictional veering (hatched area) for 500 m winds of 8-11 m/sec.

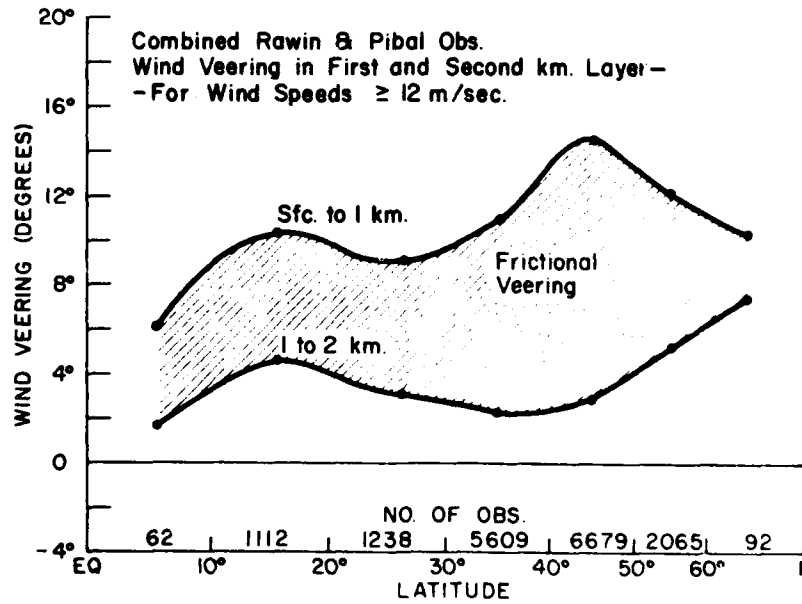


Fig. 43. Latitude distribution of frictional veering for 500 m winds ≥ 12 m/sec.

Preceding page blank

WIND VEERING (Deg.) by
WIND DIRECTION and LATITUDE

	Eq.-20°	20°-40°	40°-60°	GLOBAL MEAN
	<u>1 km - Sfc.</u>			
from North	8.3	-1.1	1.9	~ 3
South	14.1	20.3	26.5	~ 20
East	9.4	11.2	17.5	~ 13
West	8.0	7.1	7.9	~ 8
Annual	10.3	8.7	12.6	~ 10½
	<u>2 km - 1 km</u>			
from North	-0.8	-10.6	-7.4	~ -6
South	5.6	12.1	11.0	~ 10
East	3.8	3.0	9.8	~ 6
West	-0.3	1.1	0.3	~ 0
Annual	2.9	1.2	2.3	~ 2½
	<u>Frictional Veering (1 km - Sfc.) - (2 km - 1 km)</u>			
from North	7.5	11.7	9.3	~ 9
South	8.5	8.2	15.5	~ 10
East	5.6	8.2	7.7	~ 7
West	8.3	6.0	7.6	~ 8
Annual	7.4	7.5	10.3	~ 8

Table 7.

Veering vs. Season and Latitude. Figs. 45-48 show the latitude variation of 1st and 2nd km veering by season and Fig. 49 portrays 1st km 'frictional veering' in combination for all seasons. Table 9 more explicitly lists these seasonal veering values by 20° latitude intervals. Table 10 shows the 1st and 2nd km perpendicular component variations of veering by season.

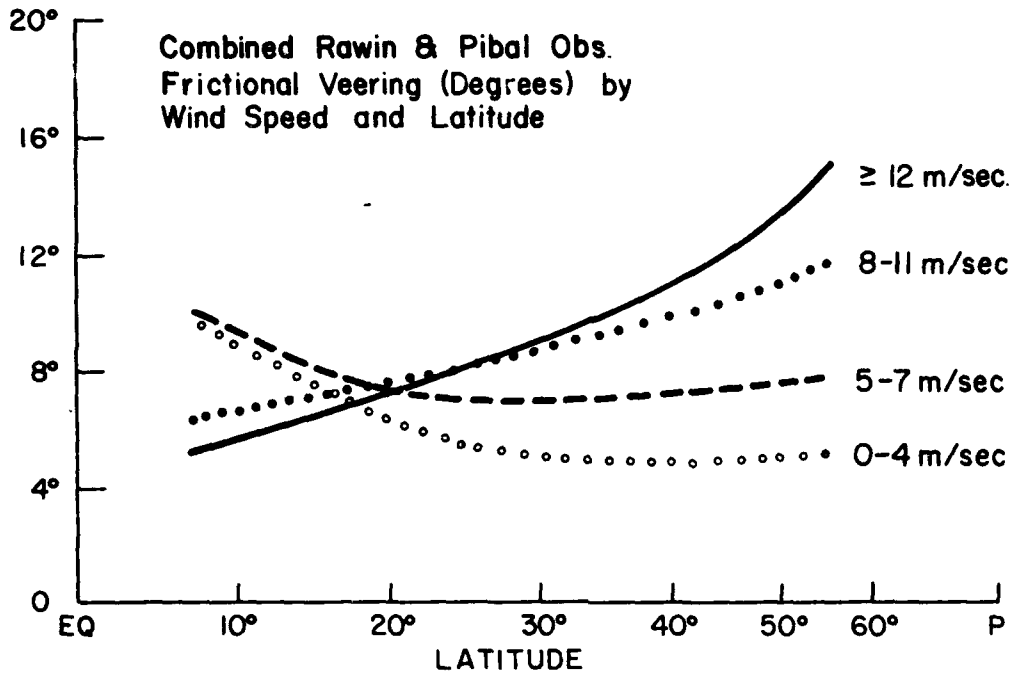


Fig. 44. Latitude distribution of frictional veering by wind speed.

Seasonal differences are, in general, not very large. The lower autumn and winter frictional veering in middle latitudes are felt to be partly related to increased vertical lapse rate instability brought about by cold air moving over warmer water in the shipping lanes of the western oceans where the ship data is concentrated. Fig. 10 shows that one would expect a decrease of observed veering with increasing vertical instability.

It is thus seen that there are no large seasonal veering differences.

Conclusion. Ship observations indicate that the 1st km oceanic 'frictional veering' has no primary relationship with latitude, wind direction,

WIND VEERING (Deg.) by
WIND SPEED and LATITUDE

WIND SPEEDS m/sec	Eq.-20	20-40	40-60	GLOBAL MEAN
	<u>1 km - Sfc.</u>			
0-4 m/sec	11.2	6.7	7.7	~ 8
5-7	11.4	7.5	8.9	~ 9
8-11	9.8	8.0	12.8	~ 10
≥12	10.2	10.6	14.2	~ 12
Annual	10.3	8.7	12.6	~ 10½
	<u>2 km - 1 km</u>			
0-4 m/sec	2.3	0.3	2.4	~ 3
5-7	2.3	0.5	1.3	~ 2
8-11	3.2	-0.2	1.8	~ 3
≥12	4.4	2.4	1.0	~ 4
Annual	2.9	1.2	2.3	~ 3
	<u>Frictional Veering (1km - Sfc.) - (2 km - 1 km)</u>			
0-4 m/sec	8.9	5.4	5.3	~ 6
5-7	9.1	7.0	7.6	~ 8
8-11	6.6	8.2	11.0	~ 9
≥12	5.8	8.2	13.2	~ 9
Annual	7.4	7.5	10.3	~ 8

Table 8.

season, or with wind speed in tropical and subtropical latitudes. In westerly latitudes, strong winds veer more than weak winds. For all stratifications, the first km observed veering is observed to be about 10-11°, the second km veering about 2°. These results hold very well even at deep tropical latitudes. The lack of any observed frictional wind veering correlation with latitude is most striking and significant. This is discussed in the last section.

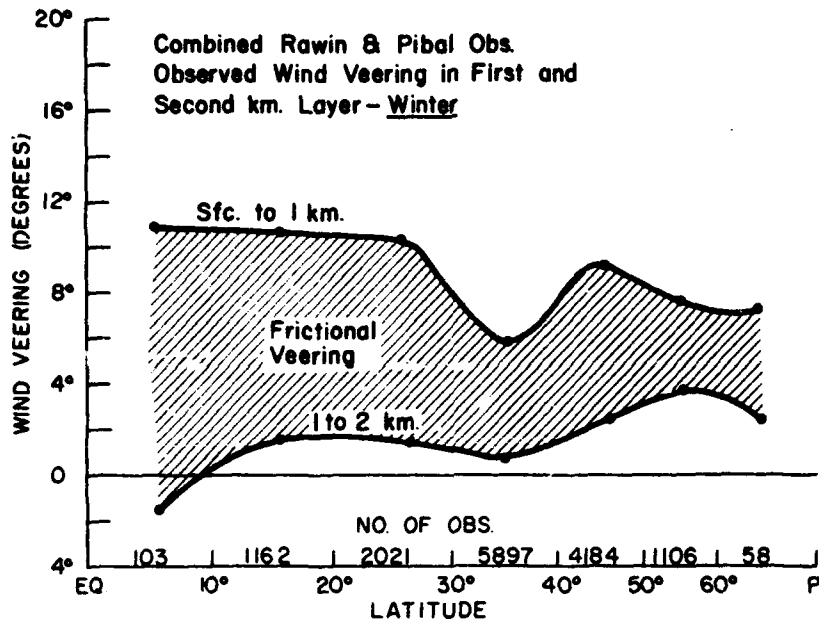


Fig. 45. Latitude distribution of frictional veering in winter.

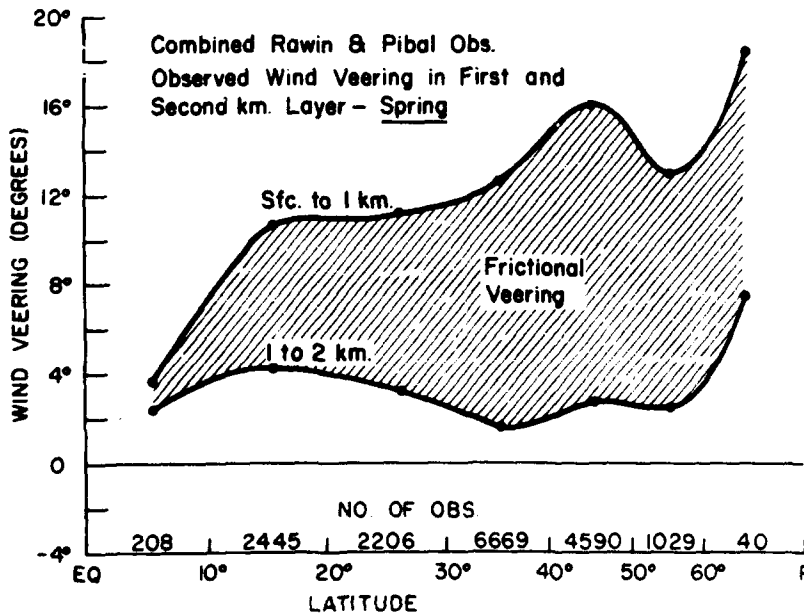


Fig. 46. Latitude distribution of frictional veering in spring.

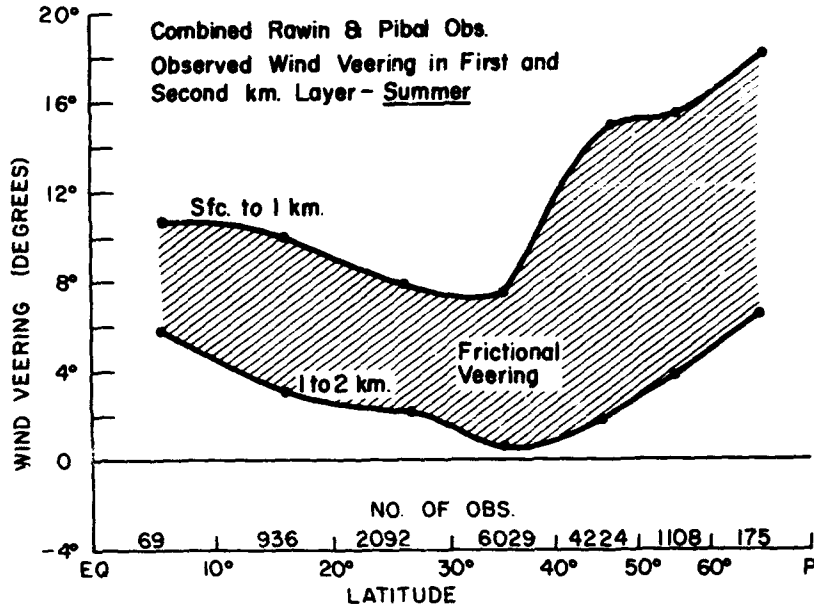


Fig. 47. Latitude distribution of frictional veering in summer.

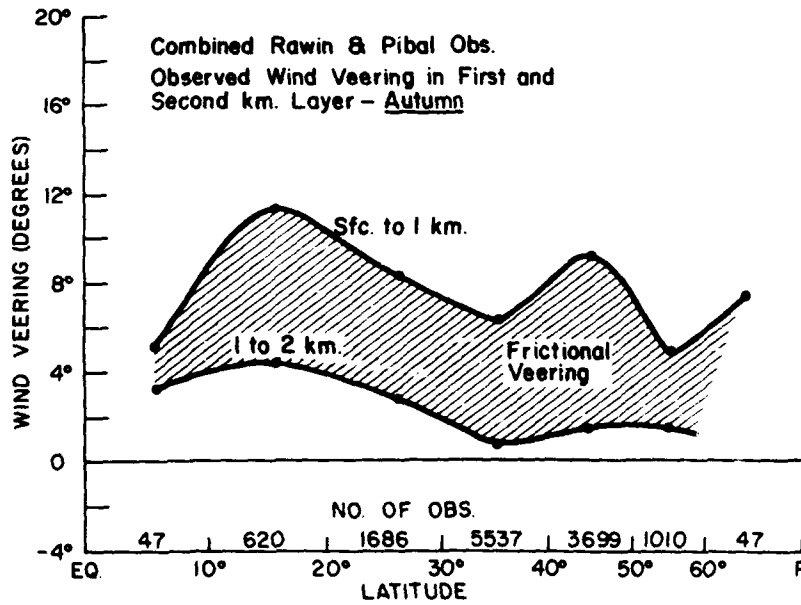


Fig. 48. Latitude distribution of frictional veering in autumn.

**WIND VEERING (Deg.) by
SEASON and LATITUDE**

	Eq-20°	20°-40°	40°-60°	GLOBAL MEAN
<u>1 km - Sfc.</u>				
Spring	10.7	12.2	16.0	~ 13
Summer	10.1	7.6	15.8	~ 11
Autumn	11.1	6.8	9.0	~ 9
Winter	10.0	6.8	11.0	~ 9
Annual	10.3	8.7	12.6	~ 10½
<u>2 km - 1 km</u>				
Spring	4.0	2.0	2.9	~ 3
Summer	2.4	0.7	2.2	~ 3
Autumn	2.2	0.8	1.7	~ 3
Winter	1.4	0.7	2.8	~ 3
Annual	2.9	1.2	2.3	~ 2½
<u>Frictional Veering (1 km - Sfc.) - (2 km - 1 km)</u>				
Spring	6.7	10.2	13.1	~ 10
Summer	7.7	6.9	13.4	~ 8
Autumn	6.9	6.0	8.3	~ 7
Winter	8.6	6.1	8.2	~ 8
Annual	7.4	7.5	10.3	~ 8

Table 9.

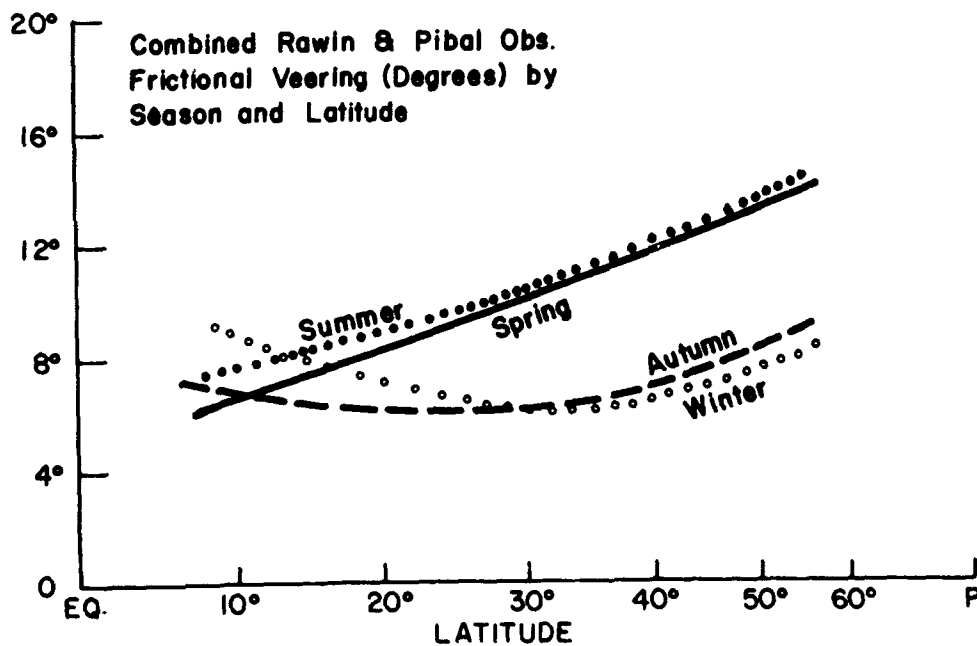


Fig. 49. Frictional veering by latitude and season.

**SHEARING OF WIND COMPONENT (m/sec) PERPENDICULAR
TO THE SURFACE WIND - positive values are veering**

	Eq.-20°	20°-40°	40°-60°	% of each layer
	<u>1 km - Sfc.</u>			
Spring	1.5	1.5	3.0	80%
Summer	1.3	1.1	2.3	
Autumn	1.4	1.0	2.0	
Winter	1.5	1.0	2.0	
Annual	1.4	1.2	2.3	
	<u>2 km - 1 km</u>			
Spring	0.6	0.3	0.5	20%
Summer	0.4	0.3	0.4	
Autumn	0.6	0.2	0.4	
Winter	0.3	0.2	0.7	
Annual	0.5	0.2	0.5	
	<u>(1 km - Sfc.) - (2 km - 1 km)</u>			
Spring	0.9	1.2	2.5	
Summer	0.9	0.8	1.9	
Autumn	0.8	0.8	1.6	
Winter	1.2	0.8	1.3	
Annual	0.9	1.0	1.8	

Table 10.

VI. DYNAMIC CONSIDERATIONS

Wind Speeds. The average speed of the ship surface winds (u_0) as measured at 10 meters (deck level) height are shown in Fig. 50. Typical values are 6-8 m/sec, less in deep tropics, more in westerly latitudes. The surface stress and kinetic energy dissipation are roughly proportional to the square and cube of the surface winds, respectively. These are also shown in Fig. 50. In the westerly latitudes these latter values are much larger than in the tropics. It will be assumed that these values are latitudinally representative of the oceans even though the data does have longitudinal bias—being concentrated along the shipping lanes. This is not felt to be a very restrictive assumption. Figs. 51 and 52 portray the vertical variation of wind speed and kinetic energy up to 2 km height by latitude.

Stress Determinations. A number of researchers have attempted direct determinations of the bulk aerodynamic drag coefficient (C_d) over the oceans in various locations. Estimates range from ~ 1 to 2×10^{-3} . Brocks and Krügermeyer (1970) and Hasse (1970) have recently discussed and presented new data and interpretation on the drag coefficients under neutral conditions. They obtain a value of $\approx 1.3 \times 10^{-3}$. Fig. 53 (from Brocks and Krügermeyer) shows no significant change of C_d with wind speed. It will thus be assumed that C_d is constant with both wind speed and latitude, even though other evidence is available to indicate a slight increase of C_d with wind speed.

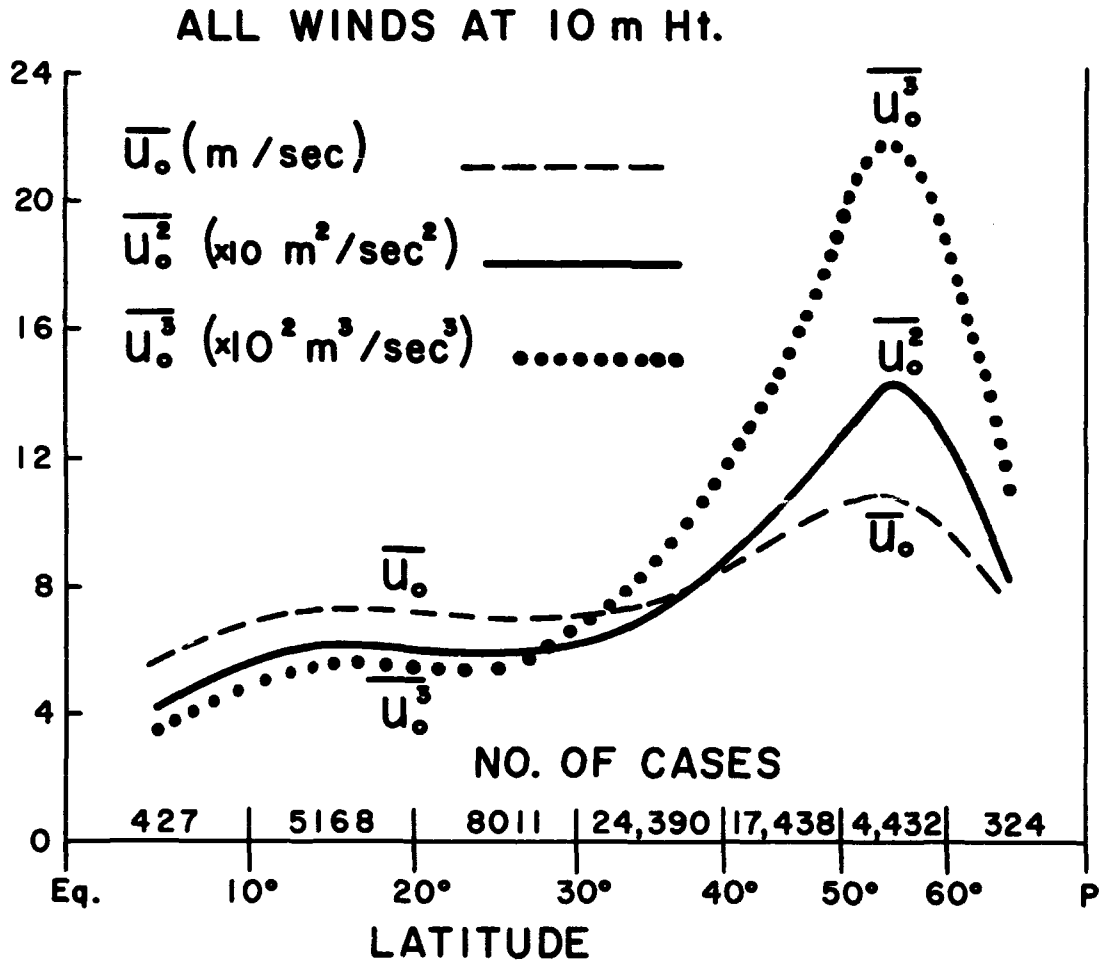


Fig. 50. Latitude portrayal of 10 meter height ship mean wind (\bar{u}_0), mean of wind squared (\bar{u}_0^2), and mean of wind cubed (\bar{u}_0^3).

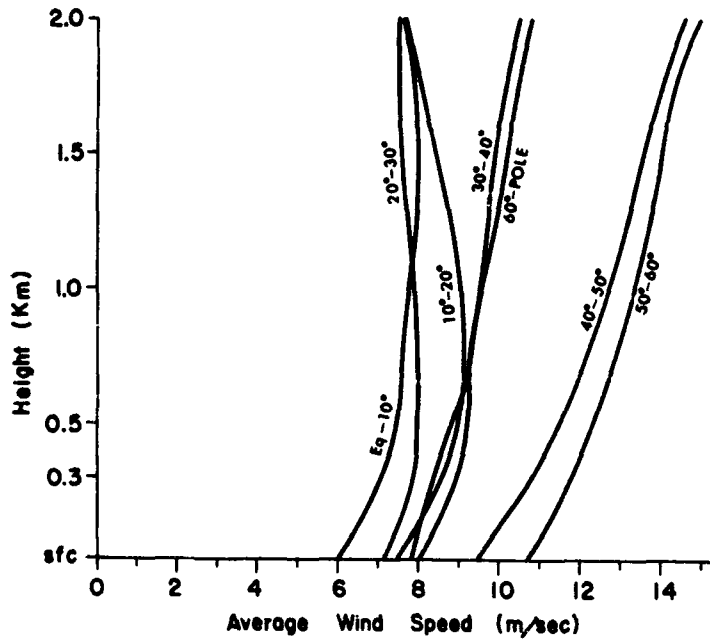


Fig. 51. Variation of wind speed in the lowest 2 km.

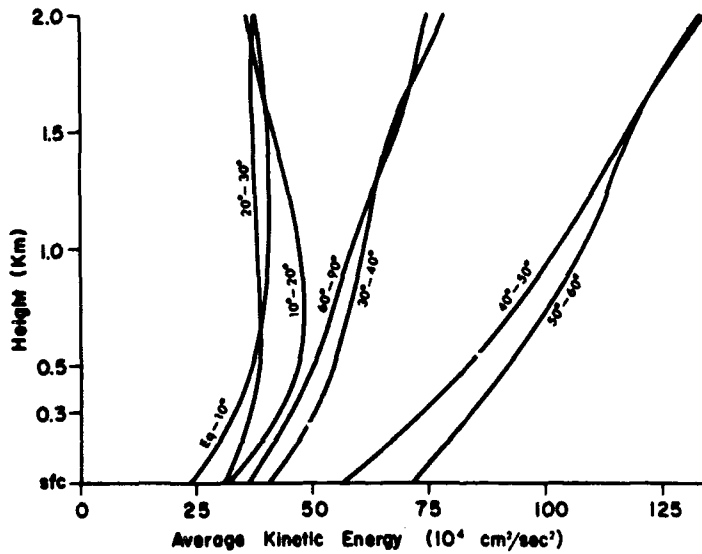


Fig. 52. Variation of kinetic energy in lowest two km.

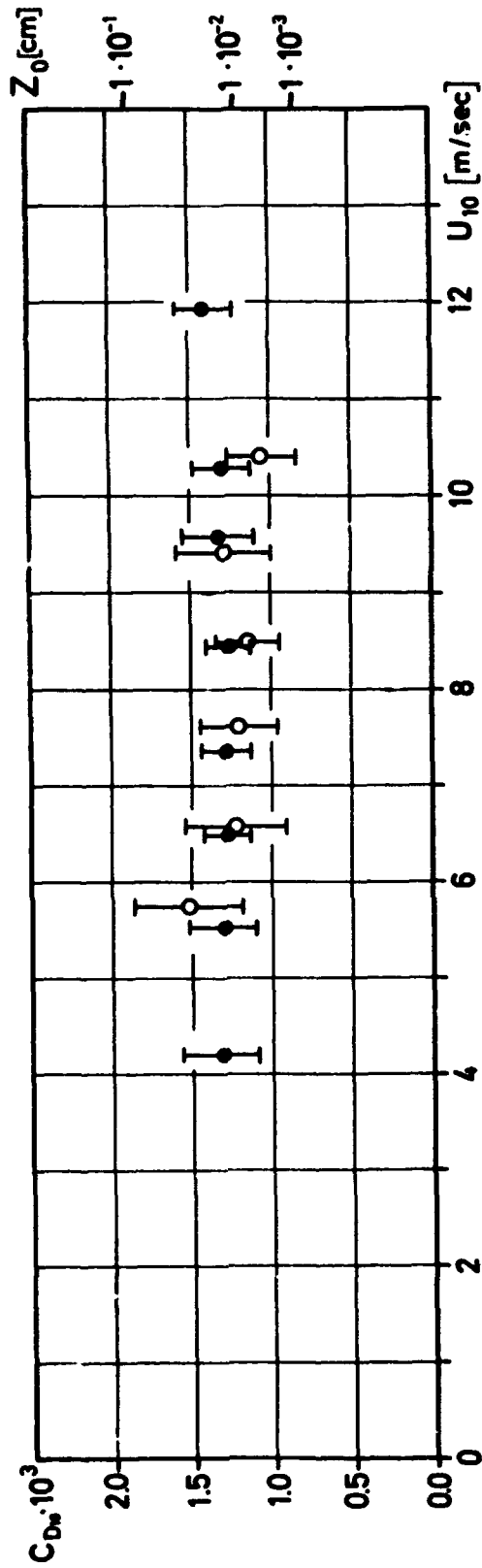


Fig. 53. Mean values and standard deviations of the drag coefficient as a function of mean wind speed (at 10 m) derived from wind profiles under neutral conditions. Dots are for the Baltic and North Sea, the circles for the equatorial Atlantic. No significant latitude difference is detected (from Brocks and Krügermeyer, 1970).

Given this value of C_d (ie. 1.3×10^{-3}) and the observed average of the square of the wind speeds at ship deck level ($\overline{u_o^2}$), the surface stress (τ_{xz_o}) can be obtained from equation (1) under the assumption of neutral lapse conditions. Thus, with ρ_o = surface density,

$$\tau_{xz_o} = C_d \rho_o \overline{u_o^2} \quad (1)$$

The latitudinal distribution of surface stress calculated this way is portrayed by the top curve of Fig. 54. Values range from ~ 0.7 to 2 dyn/cm². These estimates of stress agree quite well with the previous estimates of Priestley (1951), Hellerman (1967), Hantel (1970), and the estimates of others as reported by Malkus (1960), and Roll (1965). The bottom curve of this figure portrays the stress calculated by the geostrophic departure method defined by equation (2)

$$\tau_{xz_o} = \int_{sf_c}^{1km} \rho f (v-v_g) \delta Z \quad (2)$$

where f is the Coriolis parameter,

$(v-v_g)$ is the ageostrophic or perpendicular component of the wind (positive to the left of the wind looking downstream), and

δZ is assumed to be 1 km (ie. no ageostrophic wind at 1 km).

These latter stress values are but 10 to 50 percent of the stress calculated from (1). Equation (2) grossly underestimates the expected oceanic surface stress, especially in tropical latitudes. The observed ageostrophic component, due to frictional veering of only 10° , is too small to

account for the expected values of stress. Over land, where the typical frictional veering is $\sim 25-35^\circ$, equation (2) gives a much more realistic stress approximation.¹

Surface Ageostrophic Wind Components. Fig. 55 shows the latitude distribution of the surface or 10 meter ship deck wind (u) and the calculated geostrophic wind (u_g). The ratio of u/u_g ranges from .76 to .90. These are comparable to the estimates of other researchers. In arriving at the surface value of u_g , a constant thermal wind was assumed in the first and second km layers for westerly winds and in the first and second 500 meter layers in the trade wind belt. u_g is obtained by the downward extrapolation of wind velocity from higher levels under assumed constant baroclinicity. This will be a good approximation if no significant 1st and 2nd km (or 0-0.5 and 0.5-1.0 km for the trades) thermal wind differences are present. In the statistical average this is felt to be a reasonable assumption.

Fig. 56 portrays the latitudinal distribution of the difference between the actual and geostrophic surface wind components along $-(u-u_g)$ and perpendicular $(v-v_g)$ to the boundary layer pressure gradient. These ageostrophic components have similar magnitudes and change little with latitude.

¹ Land vs. ocean veering is discussed in a later section.

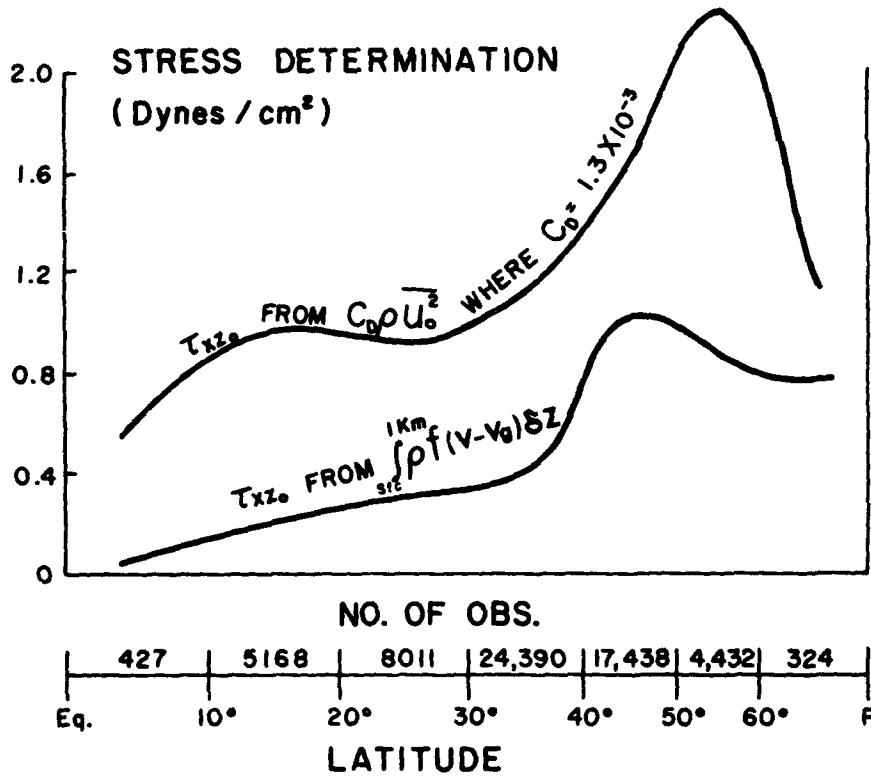


Fig. 54. Latitude distribution of stress determined by two methods if zero stress assumed to occur at 1 km height.

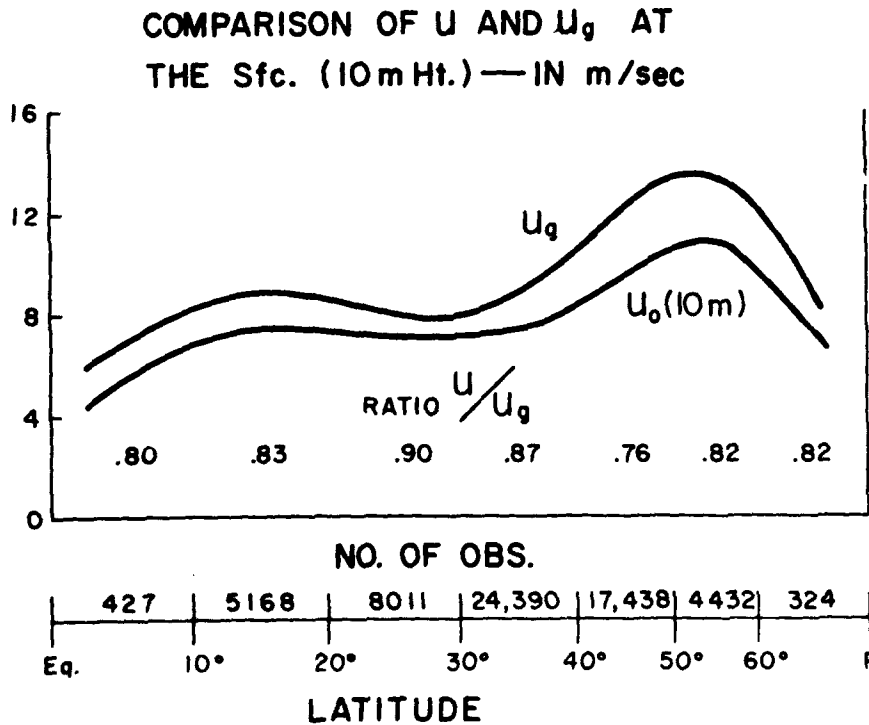


Fig. 55. Latitude distribution of the comparison of the 10 meter height ship wind with the calculated geostrophic wind at that height.

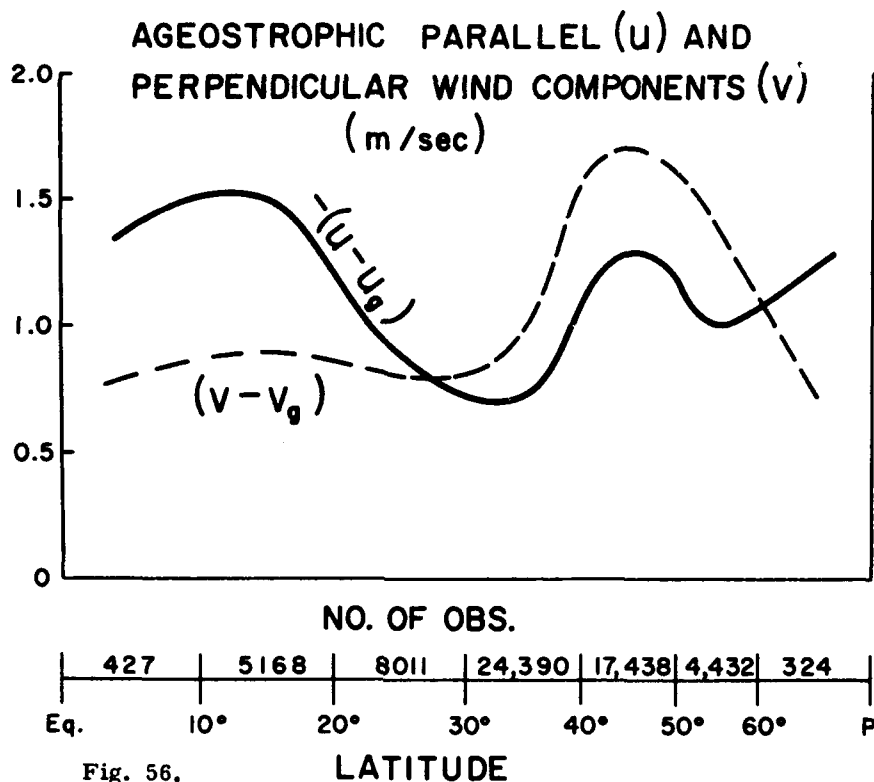


Fig. 56.

Latitude distribution of the comparison of the ageostrophic parallel $-(u-u_g)$ and perpendicular $(v-v_g)$ wind component measured at the 10 meter ship height.

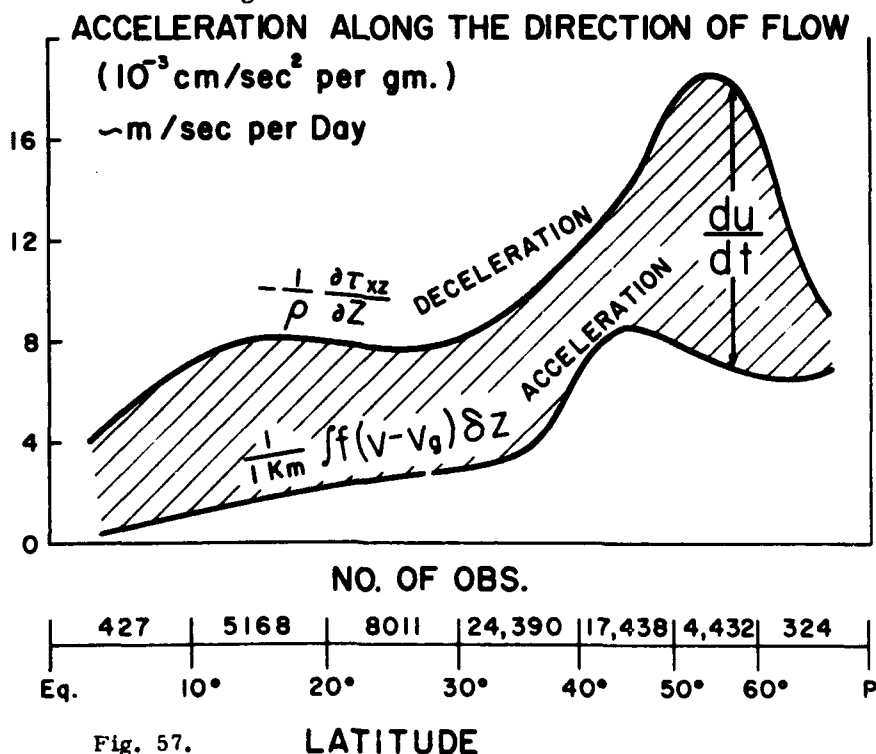


Fig. 57.

The mean lowest km accelerations along the direction of wind motion if zero stress is present at 1 km level. Note that the friction or deceleration term is much larger than the acceleration term. Most of this difference $\frac{du}{dt}$ is believed to be accounted for by momentum convergence from upper layers.

MODEL OF ZERO TURBULENT STRESS AT 1 km (\sim 900 mb)

In this section it is assumed that the turbulence stress and ageostrophic wind component decreases to zero at 1 km. These assumptions are made for simplicity. They lead to an underestimate of the ageostrophic wind component and of the kinetic energy generation if the top of the boundary layer is at a higher level.

Boundary Layer Acceleration for Zero Stress at 1 km. With the observed values of veering and stress obtained from equation (1), it is possible to calculate the total time derivative of the wind. Assuming no net curvature influences, the tangential equation of motion can be expressed as

$$\frac{du}{dt} \left(\begin{array}{l} \text{mean through} \\ \text{1st km} \end{array} \right) = \frac{1}{\Delta z} \left[f(v-v_g) \delta z + \frac{1}{\Delta z} \left[\frac{1}{\rho} \frac{\partial \tau_{xz}}{\partial z} \delta z \right] \right] \quad (3)$$

Fig. 57 shows the mean 1st km frictional deceleration $\left[\frac{1}{\Delta z} \left[\frac{1}{\rho} \frac{\partial \tau_{xz}}{\partial z} \delta z \right] \right]$ along the direction of flow and the observed boundary layer acceleration $\left[\frac{1}{\Delta z} \left[f(v-v_g) \delta z \right] \right]$ from cross-contour flow computed from the observed values of u_0 , C_d , v , v_g and with Δz equal to assumed boundary height of 1 km. A large (\sim 5 m/sec per day) deceleration ($-\frac{du}{dt}$) is obtained. This is larger than expected. For steady conditions the importance of a higher level momentum source and downward transport mechanism is clearly evident.

Kinetic Energy Dissipation-Generation for Zero Stress at 1 km.

Boundary layer kinetic energy (KE) dissipation per unit mass can be approximated by,

$$\text{KE Dissipation} = \frac{1}{\Delta z} \int_0^{1 \text{ km}} u \cdot \frac{\partial \tau_{xz}}{\rho \partial z} \delta z \quad (4)$$

where Δz is taken to be ~ 1 km and

$$C_d \text{ is } 1.3 \times 10^{-3}$$

u is the wind along the direction of flow.

Assuming that the stress decreases with height in proportion to the wind veering, the actual vertical distribution of dissipation can be obtained.

1st km kinetic energy (KE) generation per unit mass may be estimated from the formula

$$\text{KE generation} = \frac{1}{\Delta z} \int_{\text{sfc}}^{1 \text{ km}} f u (v - v_g) \delta z \quad (5)$$

Latitudinal distributions of lowest km net kinetic energy (KE) dissipation and generation for all wind classes are given in Fig. 58. Values are portrayed in watts/m². Note the large net oceanic dissipation to generation ratios, especially in the Tropics. This much larger than one (dissipation to generation) ratio is valid for all speed classes. Figs. 59-62 show this same ratio for wind speed stratifications (based on the 500 m wind) in the ranges of 0-4, 5-7, 8-11, >12 m/sec. For all wind speeds, dissipation is much larger than generation. This is different than over land areas where, as reported by Kung (1967) in a five year study over North America, the KE dissipation and generation are close to balancing.

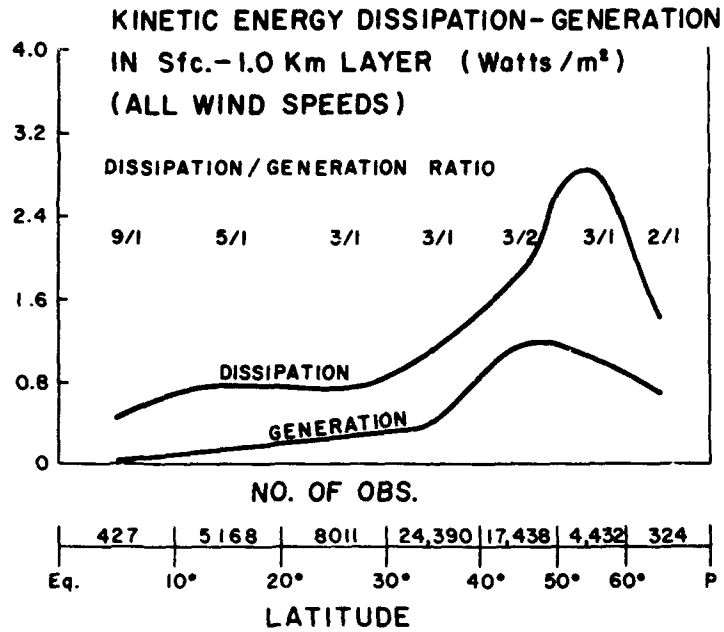


Fig. 58. Latitude distribution of the kinetic energy dissipation and generation for all wind speed values if zero stress is assumed at 1 km height.

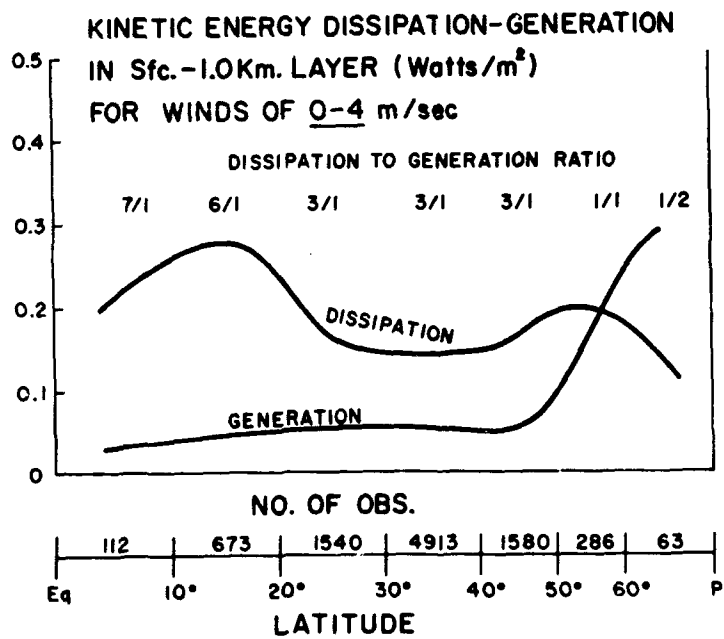


Fig. 59. Same as Fig. 58 but for 0-4 m/sec winds.

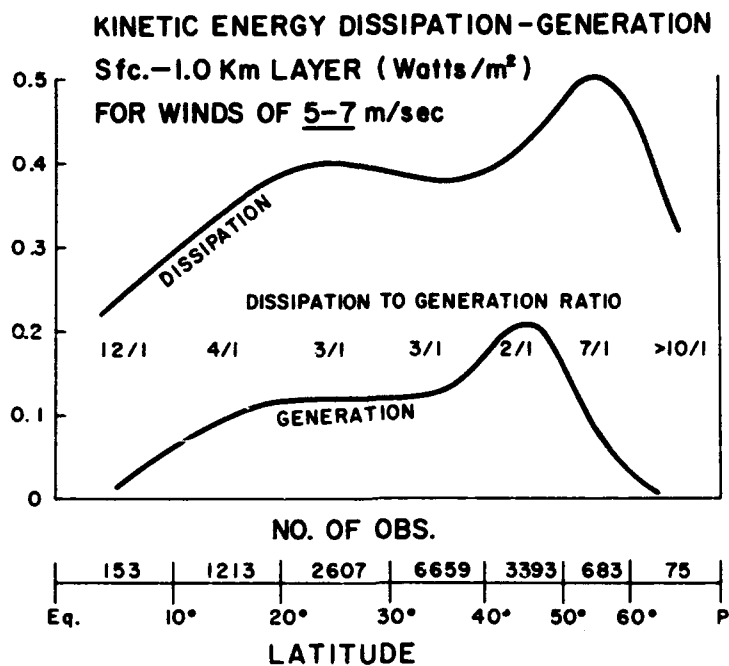


Fig. 60. Same as Fig. 58 but for 5-7 m/sec winds.

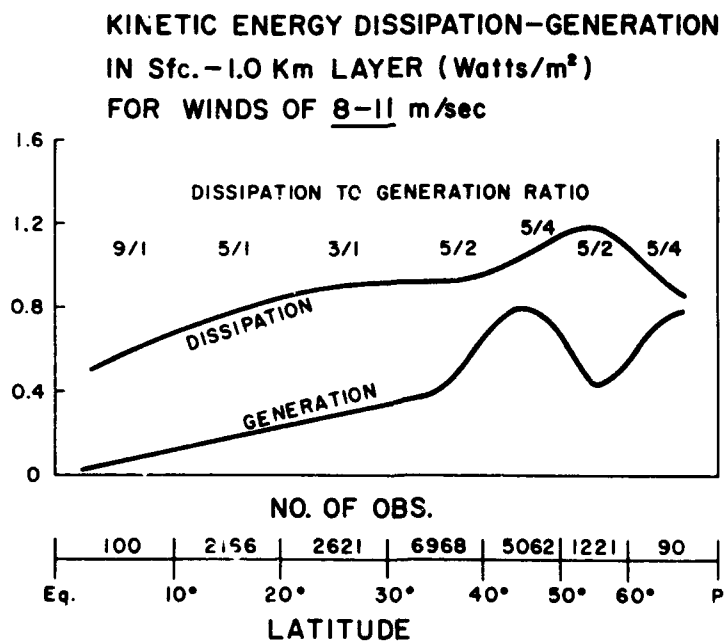


Fig. 61. Same as Fig. 58 but for 8-11 m/sec winds.

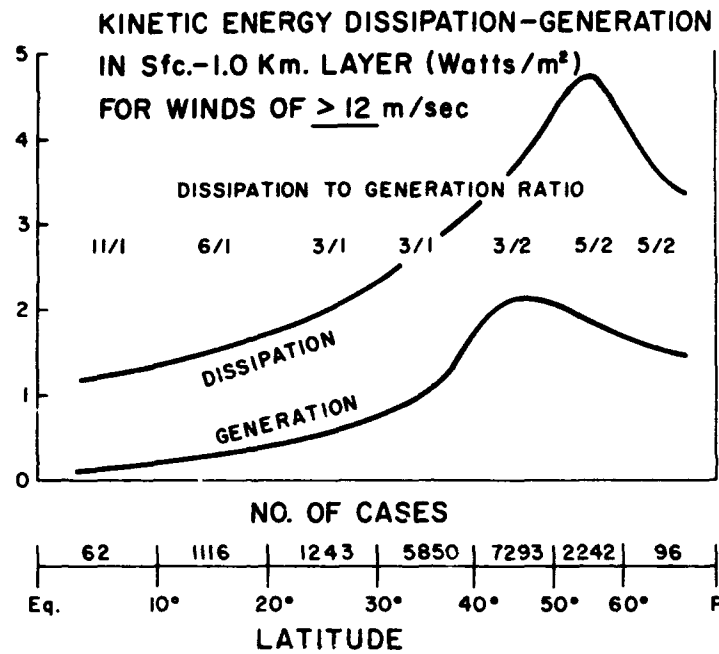


Fig. 62. Same as Fig. 58 but for wind > 12 m/sec.

The oceanic dissipation to generation ratio is especially large in the tropical latitudes where, (due to small value of f), pressure gradients are small. A typical $8-10^{\circ}$ surface cross contour flow in the tropics will generate much less KE than a similar crossing angle at higher latitudes. Table 11 portrays idealized latitudinal KE dissipation and generation for wind velocities of 5, 10, and 15 m/sec. In these calculations it has been assumed that

- 1) frictional boundary layer is one km in depth and the frictional veering at the surface is 10°
- 2) average ageostrophic component in boundary layer $(\overline{v-v_g})$ is one half the surface ageostrophic component, thus $\overline{v-v_g} = \frac{1}{2} (v-v_g)_{sfc}$
- 3) $C_d = 1.3 \times 10^{-3}$.

Table 11

Theoretical kinetic energy dissipation, and generation (in watts/m²) ratios for different wind speeds from equations (4) and (5) for assumed conditions of 10° surface frictional veering angle, $C_d = 1.3 \times 10^{-3}$, and mean veering through lowest km (\bar{v}) equal to one-half surface veering.

	LATITUDE						
	<u>Eq-10°</u>	<u>10-20°</u>	<u>20-30°</u>	<u>30-40°</u>	<u>40-50°</u>	<u>50-60°</u>	<u>>60°</u>
For $u = 5$ m/sec, $\overline{v - v_g} = .38$ m/sec							
Dissipation	.16	.16	.16	.16	.16	.16	.16
Generation	.03	.07	.12	.16	.20	.23	.26
Diss./Gen.	5.30	2.30	1.30	1.00	0.80	0.70	0.60
For $u = 10$ m/sec, $\overline{v - v_g} = .85$ m/sec							
Dissipation	1.30	1.30	1.30	1.30	1.30	1.30	1.30
Generation	.13	.31	.51	.69	.85	.99	1.11
Diss./Gen.	10.00	4.20	2.50	1.90	1.50	1.30	1.20
For $u = 15$ m/sec, $\overline{v - v_g} = 1.28$ m/sec							
Dissipation	3.37	3.37	3.37	3.37	3.37	3.37	3.37
Generation	.29	.71	1.15	1.55	1.93	2.25	2.50
Diss./Gen.	11.60	4.70	2.90	2.20	1.80	1.50	1.40

It is seen that the dissipation to generation ratio goes up with wind speed and is especially large in tropical latitudes. This is to be expected where dissipation is proportional to the cube of the wind speed and generation to fv . If the frictional veering angle is approximately constant with latitude, then the dissipation-generation ratio of $\sim u^2/fv$ must be quite substantial at low latitudes where f is small.

In a physical sense air in motion in the boundary layer near the equator should be retarded as much (and transfer as much momentum and kinetic energy to the surface) as boundary layer air at higher latitudes. The smaller tropical pressure gradients, however, prevent a compensating generation as large as that possible at higher oceanic latitudes. Over land, where the crossing angles are closer to 30° rather than 10° , a much closer (at least in middle-latitudes) dissipation to generation balance is possible. Fig. 63 portrays the net 1st km oceanic KE dissipation with latitude and a comparison with Kung's (1967) five-year average KE dissipation over North America at 00Z and 12Z. In middle latitudes the land and oceanic dissipation energies are comparable.

Model of Zero Turbulent Stress at 2 km (~ 800 mb). About 20 percent of the wind veering in the lowest 2 km occurs in the 2nd km layer. If it is assumed that the stress decreases as the wind veering and that the level of zero mechanical turbulent stress is at two km (~ 800 mb) rather than one km (~ 900 mb), then the lowest km layer dissipation has been overestimated by about 20 percent if the decrease of stress is directly related to the magnitude of wind veering. The mag-

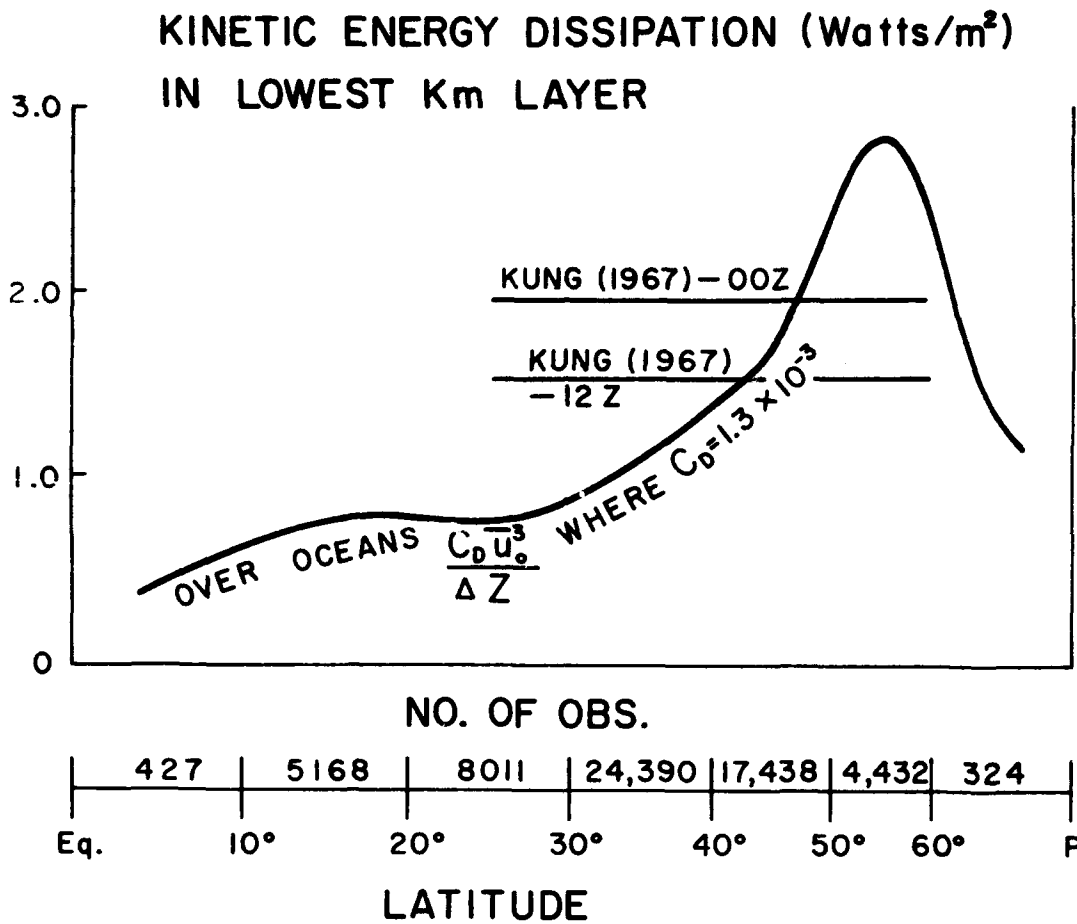


Fig. 63. Net kinetic energy dissipation in the lowest km over the oceans by latitude and comparison with values of Kung at 00Z and 12Z over the North American continent.

nitude of the generation has similarly been underestimated by about 20%-25%. This model of the zero mechanical stress at 2 km rather than 1 km leads to a decrease of the deceleration to acceleration and dissipation to generation ratios of about 45%-50%. Dissipation to generation ratios (similar to the previous figures) based on a 2 km layer top of the boundary layer for the various wind speeds are shown in Figs. 64-68. Even though these ratios are decreased, they remain substantially larger

KINETIC ENERGY DISSIPATION-GENERATION
 IN SFC-1.0 Km. LAYER IF ZERO STRESS
 AT 2.0 Km. (ALL WIND SPEEDS)

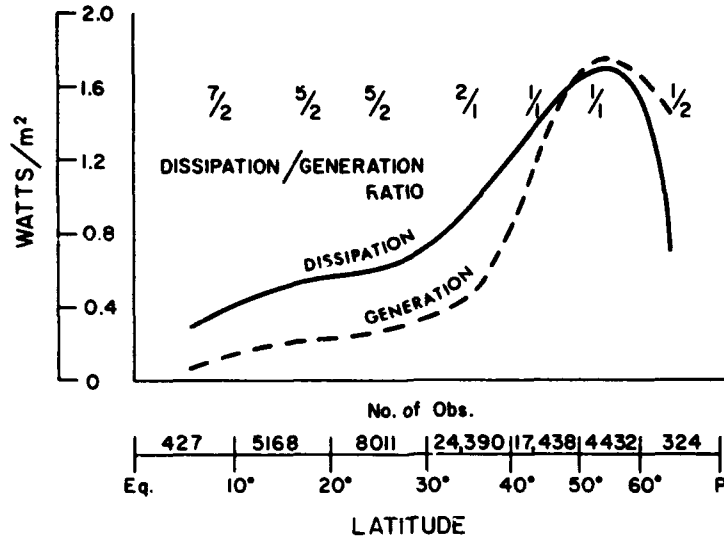


Fig. 64.

KINETIC ENERGY DISSIPATION-GENERATION
 IN SFC-1.0 Km. LAYER IF ZERO STRESS
 AT 2.0 Km. (0-4 m/sec WINDS)

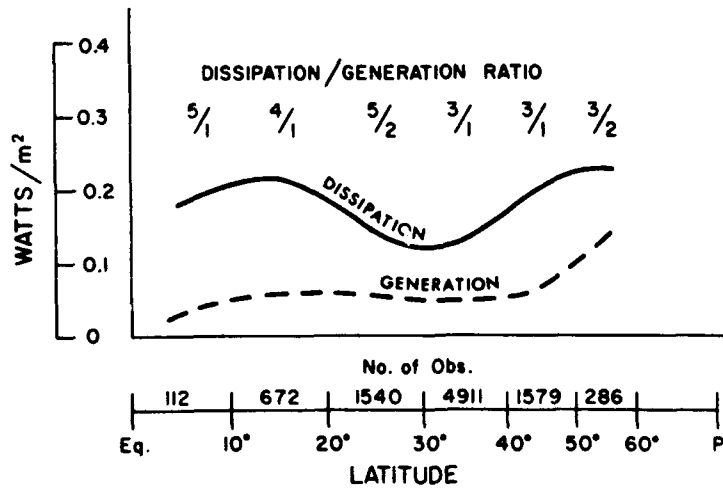


Fig. 65.

KINETIC ENERGY DISSIPATION-GENERATION
IN SFC-1.0 Km. LAYER IF ZERO STRESS
AT 2.0 Km. (5-7 m/sec WINDS)

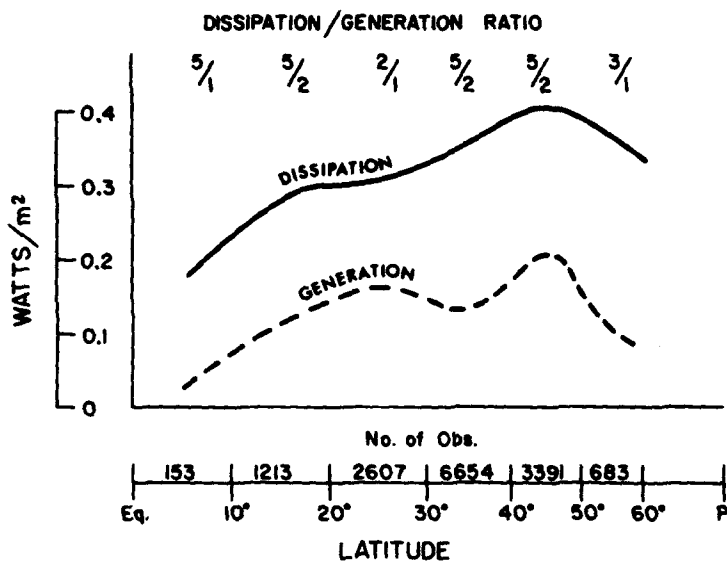


Fig. 66.

KINETIC ENERGY DISSIPATION-GENERATION
IN SFC-1.0 Km. LAYER IF ZERO STRESS
AT 2.0 Km. (8-11 m/sec WINDS)

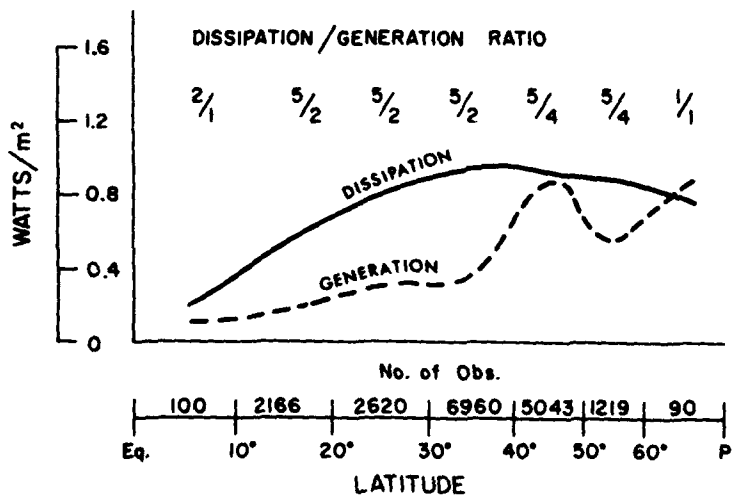


Fig. 67.

KINETIC ENERGY DISSIPATION-GENERATION
IN SFC-1.0 Km. LAYER IF ZERO STRESS
AT 2.0 Km. (>12 m/sec WINDS)

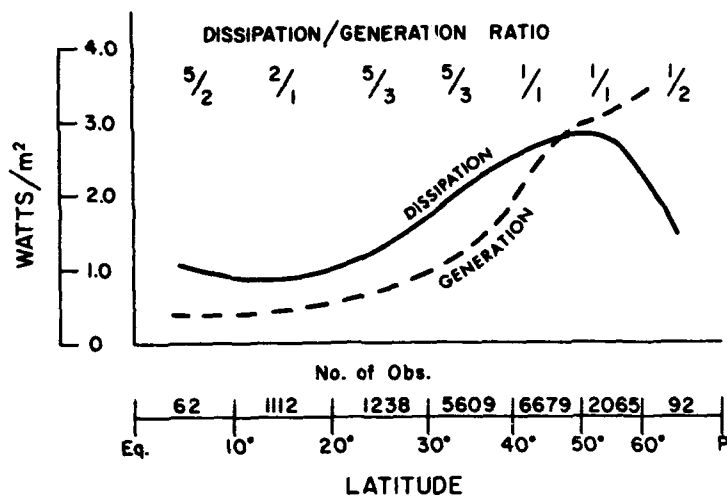


Fig. 68.

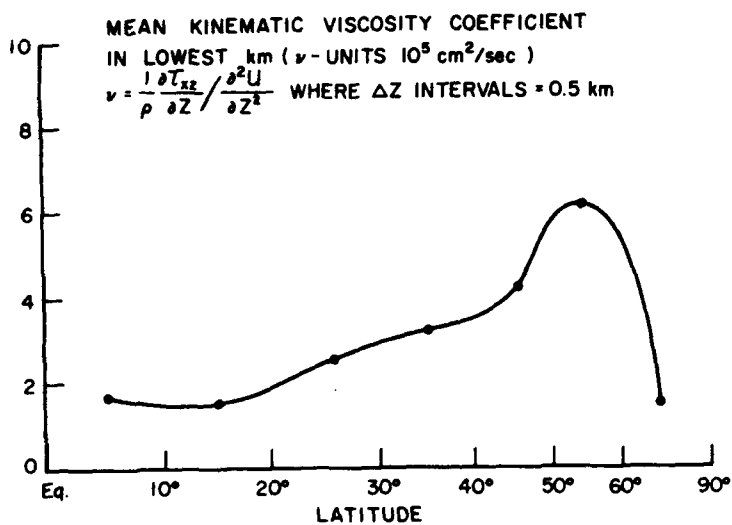


Fig. 69. Kinematic eddy viscosity coefficient required for observed stress gradient and vertical wind shear gradient in the lowest km layer.

than one in the tropics. In the middle latitudes, a more balanced dissipation to generation ratio is obtained.

Ocean vs. Land Frictional Veering. Mid-latitude and subtropical land areas show typical wind veering in the 1st km layer--not of 8° - 10° as observed over the oceans, but, as shown by Bonner and Smith (1967), Kung (1967), and Gray (1968) values of 25° - 30° --about three times larger than oceanic values. The Bonner and Smith study consisted of 22 Asian and 15 U.S. stations for winter and summer. 12,896 soundings were involved. The average veering in the 1 km layer was 29.7° . The boundary layer kinetic energy generation observations of Kung (1967) require an average lower km wind veering of ~ 25 - 30° . The author's previously undocumented land veering study consisted of a 12 month composite of the average difference of crossing angle of winds with pressure-height lines at the surface and 850 mb over the eastern half of the U.S. Approximately 12,000 values were involved. The average veering difference between the surface and 850 mb levels amounted to ~ 25 - 30° . See Table 12.

Middle latitude dissipation to generation ratios over land and ocean are $\sim \frac{1}{1}$ and $\frac{1}{3}$ respectively. Are these large land frictional veerings due primarily to higher land drag coefficient? Additional p. b. l. observational research is presently going on at Colorado State University (Hoxit, 1972) to try to better understand these land-ocean differences.

Estimated Viscosity Coefficient. From the calculated stress of equation (1) and the observed derivative of vertical shear in the bound-

Table 12

FRictional Wind Veering Over Land

Bonner and Smith (1967)

22 Asian and 15 U. S. stations. Winter and summer observations, 12,896 soundings.

Average veering in 1 km layer 29.7°

Kung (1967)

5 years observations over N. Am. To obtain observed kinetic energy generation, frictional veering must be in the range of 25°-35°.

Gray (1969)

12-month composite of the average difference of crossing angle of winds with pressure-height lines at the surface and 850 mb ht. Approximately 12,000 observations. Average difference came to 30°.

ary layer, it is possible (using 500 m shear gradients) to make an estimate of the mean oceanic p. b. l. kinematic eddy viscosity coefficient

(ν)

$$\nu = \frac{\partial \tau_{xz}}{\rho \partial z} / \frac{\partial^2 u}{\partial z^2} \quad (6)$$

Fig. 69 shows the latitudinal estimate of this coefficient in units of $10^5 \text{ cm}^2/\text{sec}$. These values are within the central range of previous estimates.

VII. DISCUSSION

Conceptual View of Oceanic Planetary Boundary Layer. The author views the p. b. l. as being primarily composed of mechanically-driven gust-scale eddies (\sim 50-500m size) whose density and magnitude decrease throughout the layer. Where cumulus clouds are present, larger scale eddies (1-10 km) can exist and extend to high levels, as portrayed in Fig. 70. The purely mechanical influences of the oceanic p. b. l. can be viewed as typically extending up to about one km height (\sim 900 mb).

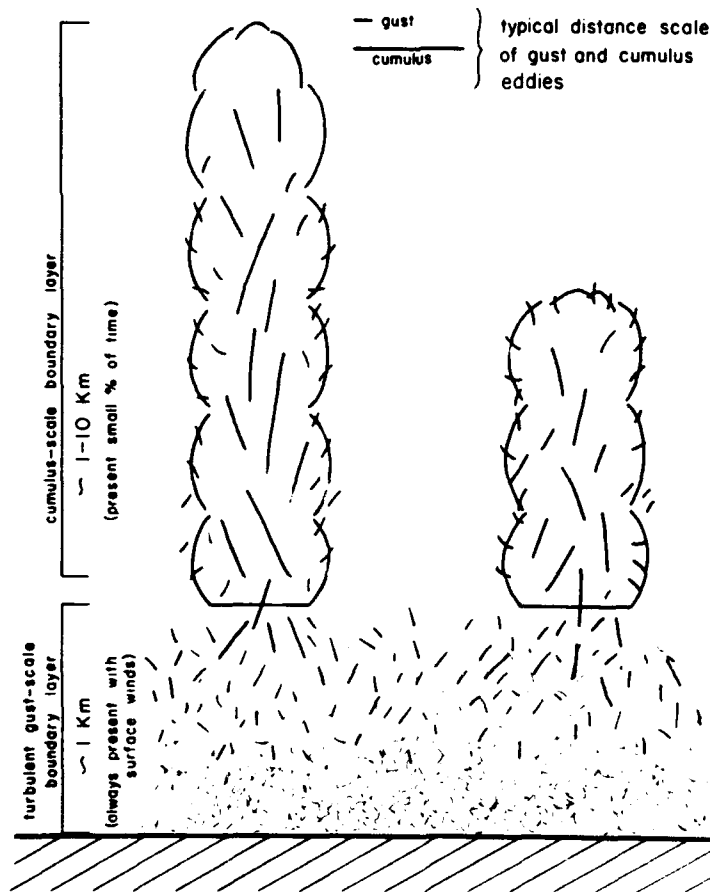


Fig. 70. Idealized view of the decrease of turbulent eddies with height and without cumulus clouds.

A diurnal p.b.l. height variation as is present over land (due to diurnal buoyancy and wind variations) is not found over the ocean. Where cumulus convection (i. e., moist processes are allowed for) oceanic p.b.l. can extend to higher levels. Cumulus clouds can distribute surface momentum to higher levels than the dry (and thus stable) purely mechanical turbulence processes are able to do. This does not negate the idealized view of a mechanical boundary layer of about 1 km height, however. Cumulus clouds occupy only a small percent of the ocean area. The cumulus clouds' net influence on altering the mechanical stress level over the oceans (except when intense convection and large vertical shears are present) is probably not very great. For these reasons, the concept of a general one km surface turbulence boundary layer is felt to be "statistically" valid.

Required Downward Transport from Higher Levels. It is clearly seen (if these observations are correct) that the oceanic p.b.l. (especially in the tropics) is not a self-contained momentum and kinetic energy system. The lowest km layer is continually running itself down. Replacement kinetic energy must come from higher levels, not by gust-scale transfers but by meso and synoptic scale clear air sinking motions, as pictorially visualized in Fig. 71, or by some other processes such as cumulus (or Cb) downdraft (Zipser, 1969) transfers. It may also be possible for vertical transports to be accomplished by cumulus (or Cb) induced gravity waves.

VERTICAL TRANSPORT OF HORIZONTAL MOMENTUM
TO OCEAN SURFACE

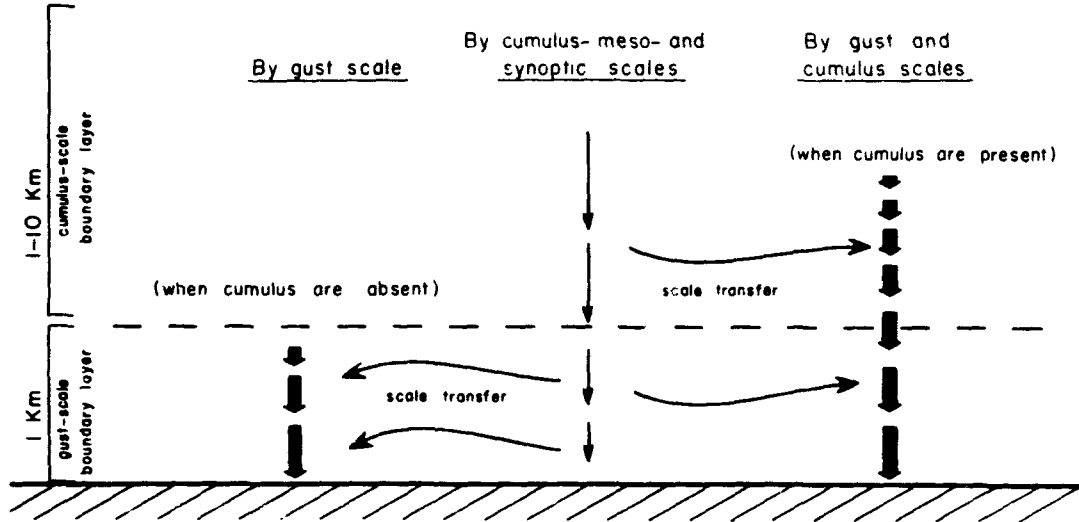


Fig. 71. Idealized view of the downward transfer of momentum by the different scales of motion.

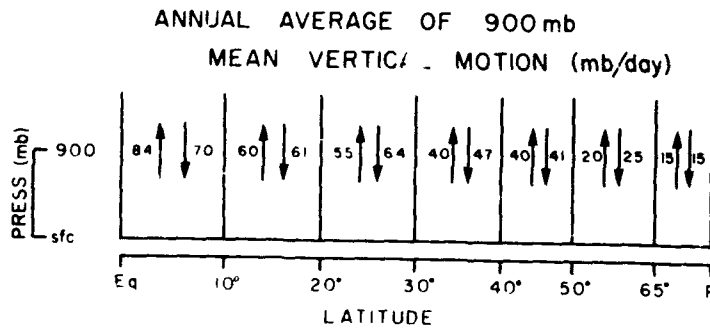


Fig. 72. Required latitudinal average up-moist and down-dry vertical circulation at the 1 km level required to explain the observed rainfall and the net heat losses by radiation and evaporation as discussed by Gray (1971).

These larger scale downward vertical transfers are believed to occur in association with the required up-moist and down-dry vertical circulations necessary to produce the rainfall and balance the net lower tropospheric radiational and evaporational cooling. The author (Gray 1971) has previously discussed this required up-moist and down-dry vertical circulation whose magnitude in mb/day is shown in Fig. 72. The required down-dry or clear air sinking will replace a substantial portion of the p.b.l. air every day, especially in tropical and subtropical latitudes. Fig. 73 is an idealized view of the typical kinetic energy balance occurring at tropical and middle latitude locations. This was determined as a compromise between assuming a one and two km zero stress height.

Depth of the Boundary Layer. The self-contained or steady boundary layer theories (Ekman, 1905 or Charney, 1969) require that the p.b.l. frictional dissipation be balanced by an equal cross contour flow. Where pressure gradient becomes small, as where one approaches the equator, these theories require the depth of the boundary layer to increase so the weaker cross-contour flow can act over a larger vertical depth and still balance the surface dissipation. The observations summarized in this report do not show a general increase in the thickness of the boundary layer as one approaches the equator. Rotation appears not to be a crucial parameter in determining the depth of the p.b.l. And why should it? The author believes that the depth of the boundary layer is primarily determined by the intensity of gust-scale kinetic

IDEALIZED KINETIC ENERGY (KE) BUDGET
OF LOWER Km LAYER OVER THE OCEANS
(arbitrary units)

	$\frac{\delta(KE)}{\delta t}$	$+\nabla \cdot \nabla KE$	$\frac{\delta \omega KE}{\delta p}$	$= -\nabla \cdot \nabla \frac{p}{\rho}$	$+ \nabla \cdot \nabla F$
MID-LATITUDES (30°-60°)	~0	~0	~-4	= ~4	~-8
TROPICS (5°-25°)	~0	~0	~-3	= ~1	~-4

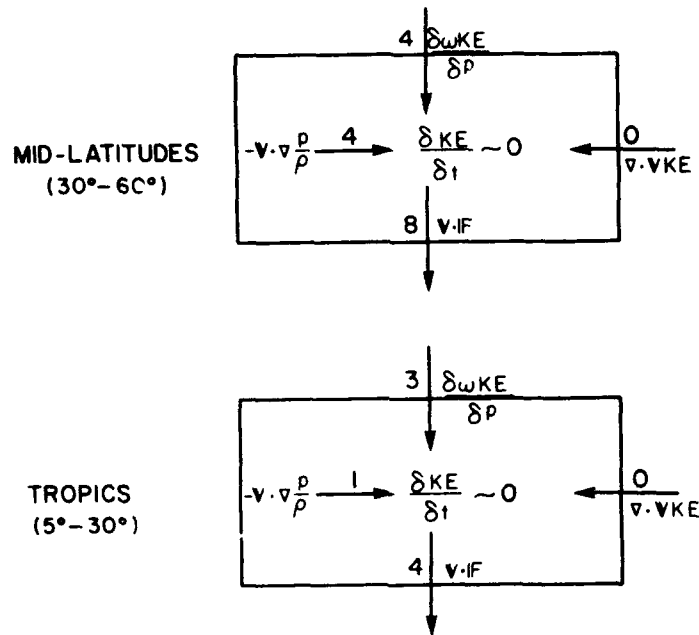


Fig. 73. Idealized view of Kinetic Energy (KE) budget in the lowest km over the oceans - arbitrary units.

energy and by the vertical stability. These factors are not related to latitude.

If the p. b. l. is not a self-contained momentum-energy system, there is no reason why a systematic latitude variation need occur. Why should the mode of turbulent interface momentum transfer from atmosphere to surface vary with latitudes? Do the turbulence eddies know at what latitude they exist?

Vertical lapse rates in the ocean planetary boundary layer are typically 0.6-0.8 of the dry adiabatic values. This means that the turbulence eddies (rising at the dry adiabatic rate) must continually act against a stable environment. The higher they go, the more negative is their buoyancy. This vertical stabilizing acceleration of the environment (A_z) may be expressed as a function of height (z) as

$$A_z = g \int_{\text{sfc}}^{z_T} \frac{(\gamma_d - \gamma_a)}{T} \delta z \quad (7)$$

where γ_d, γ_a = dry and actual lapse rates

z_T = top of p. b. l. (level at which $\overline{u'w'}$ approaches zero, where u' and w' are horizontal and vertical turbulent eddies.

Assuming the following mean layer values of actual lapse rate (γ_a) and average temperature (\bar{T})

<u>Layer (km)</u>	<u>(γ_a)</u>	<u>\bar{T}</u>
0 - 0.5	.8 γ_d	290
0.5 - 1.0	.7 γ_d	287
1.0 - 1.5	.6 γ_d	284
1.5 - 2.0	.6 γ_d	281

the mean value of A_z (in cm/sec^2 per gm) through these layers is

<u>Layer</u>	<u>\bar{A}_z</u>
0-0.5 km	1.8
0.5-1.0 km	6.4
1.0-1.5 km	13.0
1.5-2.0 km	20.6

The vertical stabilizing energy may then be expressed as

$$E_z \text{ (vertical stabilizing energy)} = \int_{\text{sfc}}^{z_T} A_z \delta z = \bar{A}_z (z_T - z_{\text{sfc}}) \quad (8)$$

The values of E_z (in $10^5 \text{ cm}^2/\text{sec}^2$ per gm) at various heights (for these A_z values) are

<u>Height (km)</u>	<u>E_z</u>
0.5	0.9
1.0	4.1
1.5	10.6
2.0	20.9

It is often observed that gustiness of surface wind speeds causes fluctuations from about half to one-and-a-half times the mean wind speed. The typical fluctuation of wind with mean speed of 5, 10, and 15 m/sec may be thought of as being in the range of about 2-1/2 to 7-1/2 m/sec, 5 to 15 m/sec, and 7-1/2 to 22-1/2 m/sec respectively. Assuming (for rough magnitude considerations) that the typical gust-scale horizontal turbulent kinetic energy ($1/2 \overline{u'^2}$, where u' is a wind eddy and the bar — indicates a long time average), is equal to one-half and one times the kinetic energy (KE) of the mean flow or ($1/2 \overline{u'^2} = 1/4 \overline{u}^2$ and $1/2 \overline{u}^2$), then the turbulent kinetic energy (in $10^5 \text{ cm}^2/\text{sec}^2$ per gm) is for various mean wind speeds:

<u>u (m/sec)</u>	Turbulent KE	
	<u>if $1/4 \overline{u}^2$</u>	<u>if $1/2 \overline{u}^2$</u>
5	0.6	1.2
10	2.5	5.0
15	5.6	11.2
20	10.0	20.0

Assuming the mixing length hypothesis to be valid to the extent that the horizontal ($\overline{1/2 u'^2}$) and vertical ($\overline{1/2 w'^2}$) kinetic energies are about the same, one might equate the horizontal turbulent kinetic energy to an equal restrictive buoyant energy height; i. e., E_z (ht) turbulent KE. This height will be called the top of the mechanical turbulent p. b. l. It is the height above which surface generated wind eddies cannot penetrate due to buoyant damping. When this is done for the above assumed kinetic energies, the following stabilizing restrictive heights are obtained:

<u>u (m/sec)</u>	Height (km)	
	<u>Turb. KE = $1/4 \bar{u}^2$</u>	<u>Turb. KE = $1/2 \bar{u}^2$</u>
5	0.4	0.7
10	0.7	1.1
15	1.1	1.5

In active convective situations where the surface wind speeds are strong and increase sharply through the troposphere, the top of the p. b. l. should be expected to go higher than 1 km. When wind speeds decrease with height in the lower troposphere, as in the trade winds, the $u'w'$ correlation in cumulus clouds will be of opposite sign to the surface $u'w'$ eddy correlation, and a cross-over or zero stress height should be readily observed at low levels.

Conclusion--The height of the p. b. l. can be specified in a general sense by vertical stability and turbulence intensity arguments by themselves without resort to rotation or steady state assumption. The in-

formation of Figs. 40-43 does indicate an increase of the mechanical boundary layer thickness with increase of wind speed. Other data currently being evaluated by Hoxit (1972) over land also are showing similar p. b. l. height variations with similar stability and wind speed changes.

Importance of Oceanic Boundary-Layer Frictional Veering and Relation to CISK Mechanism. The magnitude of, and relevance of, the first km frictional wind veering over the oceans has been open to some misinterpretation. Charney and Eliassen (1964), Ooyama (1964), and the author Gray (1968) have proposed it as part of an important physical mechanism for the intensification of cloud clusters and tropical storms. Charney and Eliassen (1964) have chosen to call the low-level frictional forcing and the meso-scale flow instability it produces (applied to tropical storm development) Conditional Instability of the Second Kind (CISK). The CISK idea has been used as the physical basis for explaining tropical storm development and has been extensively employed in hurricane intensification models.

Some meteorologists, on the other hand, who believe in the primary importance of baroclinic as opposed to frictional forcing processes have questioned the dominant role of the CISK instability idea. They feel that it has been overly stressed. This paper does not concern itself with the entire CISK process but only with that part dealing with low-level frictional forcing.

The CISK idea implies the dual physical processes of frictional convergence and unstable feedback growth. But this kind of cumulus-broad-er scale cooperative instability only takes place with intensifying tropical clusters and storms – not a frequent phenomenon. The usual occurrences of frictionally-forced cloudiness along frontal systems, with cloud clusters, the ITCZ, etc., takes place without broader-scale flow intensification. The CISK instability connotation is not an accurate description for the frictionally-forced convergence by itself. For simplicity we might call this low-level frictionally-forced process by itself "Low-level Inflow from Frictional Turning (LIFT). This low level frictional LIFT is only part of CISK, thus

$$\text{CISK} = \text{LIFT} + (\text{Feedback Instability})$$

CISK implies both the frictional forcing and the cumulus feedback instability. It is important to note this difference. Unique tropospheric flow features above the p.b.l. must be present (i. e., low tropospheric vertical wind shears, conditionally unstable lapse rates, high middle level moisture content, etc.) for cumulus feedbacks and broader-scale flow intensification to occur. Except in the comparatively rare cases of intensifying clusters and storms, this feedback instability potential is not released. This should not be taken as a reason for denying the physical importance of the LIFT process by itself, however.

Importance of Frictionally-forced Convergence. The author believes this LIFT mechanism (at least the physical idea of it) to be a fundamen-

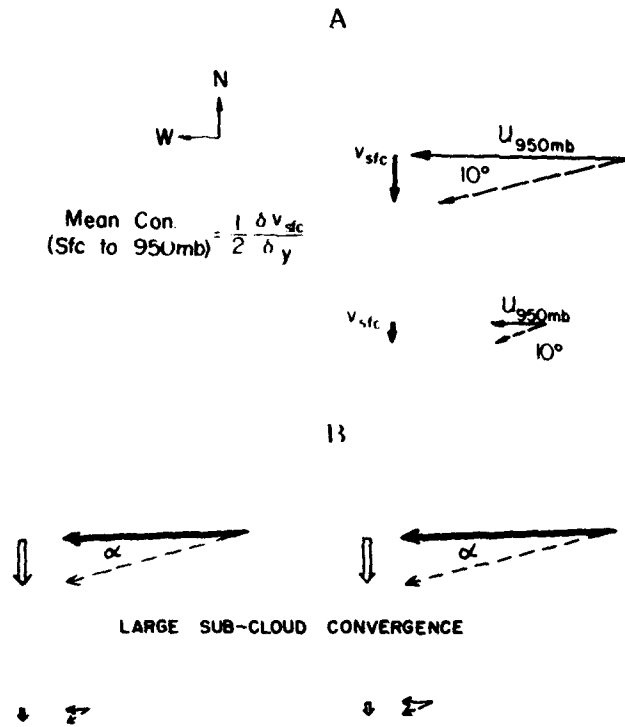


Fig. 74. Portrayal of how cyclonic shear or relative vorticity in a zonal non-divergent current at 950 mb can produce p. b. l. convergence if a frictional veering of 10° were present. It is in these shear areas when most deep cumulus convection takes place.

tally important one over the oceans in specifying the location and density of cumulus convection. A frictional wind veering in the lowest km of $\sim 10^\circ$ would lead to surface cross-isobaric flow ($\sin 10^\circ = .17$) of $\sim 15\%$ - 20% of the total wind. The average lowest km perpendicular component would be $\sim 8\%$ - 10% of the wind. In an average over the oceans, then, frictional forced lowest km convergence (C_f) would occur where there is horizontal wind shear as in Fig. 74 and would be related to the relative vorticity (Z_r) as

$$C_f \sim \frac{1}{10} Z_r \quad (9)$$

As most oceanic cumulus clouds have their bases at ~ 1 km level, a lowest km forced convergence of 10 percent of the relative vorticity would be a very significant cumulus production mechanism in regions of large horizontal wind shears such as exist along frontal zones and on the equatorial side of the Trades. It is no mere coincidence that it is in these regions where the majority of the deep-cumulus are located.

Conclusion--There is a significant (but not large) frictional wind veering in the p. b. l. over the oceans. An important purpose of the GATE and GARP programs should be a more exact quantitative specification of this physical process.

Further Work. The author will next attempt to stratify this observational data by longitude and vertical stability and will investigate veering at higher levels. He will also obtain a larger statistical sample on the veering closer to the equator. Extensive data stratifications are also proceeding over land areas so that better land-ocean comparisons can be made.

ACKNOWLEDGMENTS

This research has been financially supported by the U.S. Navy Weather Research Facility and by the National Science Foundation. The author is grateful for the assistance rendered him by Messrs. R. Hoxit, B. Mendenhall, E. Buzzell, and R. López who helped the author with decisions and with the data collections and stratifications. Mr. L. Kovacic, Mrs. B. Brumit and Mrs. G. Vloyantes performed the drafting and typing.

Much of this research was accomplished while the author was on sabbatical leave at the Department of Meteorology, Imperial College, University of London in 1970-71. The author is grateful for discussions with the Imperial College Meteorology faculty and graduate students, particularly with Professor P.A. Sheppard, Professor R.P. Pierce and Dr. J.S.A. Green.

BIBLIOGRAPHY

- Aagaard, K., 1969: Relationship between geostrophic and surface winds at Weather Ship M. J. Geophys. Res., 74, 13, June 20, pp. 3440-3442.
- Angell, J. K., D. H. Pack and C. R. Dickson, 1968: A Lagrangian study of helical circulations in the planetary boundary layer. J. Atmos. Sci., 25 (5), 707-717.
- Atkinson, G. and J. Sadler, 1970: Mean-cloudiness and gradient-level wind charts over the oceans. Technical Report 215, Vol. II, Air Weather Service Publication.
- Blackadar, A., 1967: External parameters of the wind flow in the barotropic boundary layer of the atmosphere. Stockholm GARP Report. WMO publication.
- Bonner, W., and T. Smith, 1967: Wind Predictability Studies. Project Report (NWC TP 4475) of the Naval Weapons Center, China Lake, California. 51 pp.
- Brocks, K. and L. Krügermeyer, 1970: The hydrodynamic roughness of the sea surface. Berichte des instituts für radiometeorologie und maritime meteorologie an der Universität Hamburg. Nr. 14. (English translation with German text).
- Cattle, H., 1972: Analysis of Planetary Boundary Layer Dynamics from Observational Data. Ph. D. thesis, Imperial College, University of London (in preparation).
- Charney, J. G., 1969: What determines the depth of the planetary boundary layer in a neutral atmosphere? Okeanologia, 9 (1), 143-145.
- _____, and A. Eliassen, 1949: A numerical method for predicting the perturbations of the middle latitude Westerlies. Tellus, 1, 38-54.
- _____, 1964: Growth of the hurricane depression. J. Atmos. Sci., 21, 68-75.
- Charnock, H. J., R. D. Francis and P. A. Sheppard, 1956: An investigation of wind structure in the trades: Anegada 1953: Proc. Roy. Soc. of London, Philos. Trans. A, 249, 179-234.
- Charnock, H., and T. Ellison, 1967: The boundary layer in relation to large-scale motions of the atmosphere and ocean. Stockholm GARP Report. WMO publication.
- Clark, R. H., 1970: Observational studies in the atmospheric boundary layer. J. IRMS, 96 (407), 91-114.
- Ekman, V. W., 1905: On the influence of the earth's rotation on ocean currents. Arkiv för Matematik, Astronomi, och Fysik, 2 (11), 1-52.

- Estoque, M. A., 1970: The planetary boundary layer over Christmas Island. Mon. Wea. Rev., 99, 193-201.
- Findlater, J. et al., 1966: Surface and 900 mb wind relationships. British Meteorological Office, Sci. Paper No. 23, London, 41 pp.
- Frost, R., 1948: Atmospheric turbulence. QJRMS, 74, 316-338.
- Gordon, A. H., 1950a: The ratio between observed velocities of the wind at 50 feet and 2000 feet over the North Atlantic Ocean. QJRMS, 76, 344.
- _____, 1950b: Variation of wind with height at low levels over the sea. The Meteor. Mag., 79, 295-297.
- _____, 1952a: Angle of deviation between the winds at 50 ft. and 2000 ft. over the North Atlantic Ocean. The Meteor. Mag., 81, 59.
- _____, 1952b: The relation between the mean vector surface wind and the mean vector pressure gradient over the oceans. Geofisica Pura e Applicata, 21, 49-51.
- Gray, W. M., 1968: Global view of the origin of tropical disturbances and storms. Mon. Wea. Rev., No. 10, 96, 669-700.
- _____, 1971: The magnitude of and the fundamental role of the up-moist and down-dry vertical circulation of the troposphere. Paper presented at Seventh Tech. Conf. on Hurricane and Tropical Meteor., Barbados, W. I., Dec.
- Gregg, W., 1922: An aerological survey of the United States: Part I, results of observations by means of kites. Mon. Wea. Rev., Suppl. No. 20, 78 pp.
- Hantel, M., 1970: Monthly charts of surface wind stress curl over the Indian Ocean. Mon. Wea. Rev., October, Vol. 98, No. 10, pp. 765-773.
- Hasse, L. (trans. J. F. T. Saur), 1970: On the determination of the vertical transports of momentum and heat in the atmospheric boundary layer at sea. Oregon State University, Department of Oceanography, Technical Report 188, Reference 70-22, August.
- _____, and Wagner, V., 1971: On the relationship between geostrophic and surface wind at sea. Mon. Wea. Rev., Vol. 99, No. 4, April, pp. 255-260.
- Hellerman, S., 1967: An updated estimate of the wind stress on the world ocean. Mon. Wea. Rev., 95, 607-626.
- Hoxit, R., 1972: Dynamics of the Planetary Boundary Layer as Revealed by Observations. Ph. D. dissertation, Department of Atmospheric Science, Colorado State University (in preparation).

- Janota, P., 1971: An Empirical Study of the Planetary Boundary Layer in the Vicinity of the Intertropical Convergence Zone. Ph. D. thesis, Dept. of Meteorology, M. I. T. (in preparation).
- Johnson, W. B., Jr., 1962: Climatology of atmospheric boundary-layer parameters and energy dissipation. Studies of the Three-Dimensional Structure of the Planetary Boundary Layer, Department of Meteorology, University of Wisconsin, 125-158.
- Kraus, E. B., 1966: The influence of the oceans on atmospheric disturbances and circulations. Woods Hole Oceanographic Institution Contribution No. 1576. 84 pp.
- Kung, E. C., 1963: Climatology of the Mechanical Energy Dissipation in the Lower Atmosphere over the Northern Hemisphere. Ph. D. dissertation, University of Wisconsin, 92 pp.
- _____, 1967: Diurnal and long-term variations of the kinetic energy generation and dissipation for a five-year period. Mon. Wea. Rev., Vol. 95, No. 9, September, pp. 593-606.
- _____, 1968: On the momentum exchange between the atmosphere and earth over the northern hemisphere. Mon. Wea. Rev., 96 (6), 337-341.
- Lettau, B., 1967: Thermally and frictionally produced wind shear in the planetary boundary layer at Little America, Antarctica. Mon. Wea. Rev., 95, 627-635.
- Lettau, H. H., 1959: Wind profile, surface stress, and geostrophic drag coefficients in the atmospheric surface layer. Adv. in Geophy., 6, Academic Press, New York, 241-256.
- _____, 1967: Small to large-scale features of boundary layer structure over mountain slopes. Proc. of Symposium on Mountain Meteorology. Colorado State University, Department of Atmospheric Science, Research Paper No. 122.
- _____, and B. Davidson, 1957: Exploring the Atmosphere's First Mile. 2 vols., Pergamon Press, N. Y., 344 pp.
- Lettau, et al., 1962: Studies of the Three-dimensional structure of the planetary boundary layer. University of Wisconsin, Department of Meteorology, Final Report, October, 232 pp.
- Madden, et al., 1971: Rawinsonde Data Obtained during the Line Islands Experiment. Vol. II. NCAR Technical Notes TN/STR-55.
- Malkus, J. S., 1960: The air and sea in interaction. Woods Hole Oceanographic Institution, November, 349 pp.
- Mendenhall, B. R., 1967: A Statistical study of the Frictional Wind Veering in the Planetary Boundary Layer. Atmos. Sci. Paper No. 116, Colorado State University, Fort Collins.

- Estoque, M. A., 1970: The planetary boundary layer over Christmas Island. Mon. Wea. Rev., 99, 193-201.
- Findlater, J., et al., 1966: Surface and 900 mb wind relationships. British Meteorological Office, Sci. Paper No. 23, London, 41 pp.
- Frost, R., 1948: Atmospheric turbulence. QJRMS, 74, 316-338.
- Gordon, A. H., 1950a: The ratio between observed velocities of the wind at 50 feet and 2000 feet over the North Atlantic Ocean. QJRMS, 76, 344.
- _____, 1950b: Variation of wind with height at low levels over the sea. The Meteor. Mag., 79, 295-297.
- _____, 1952a: Angle of deviation between the winds at 50 ft. and 2000 ft. over the North Atlantic Ocean. The Meteor. Mag., 81, 59.
- _____, 1952b: The relation between the mean vector surface wind and the mean vector pressure gradient over the oceans. Geofisica Pura e Applicata, 21, 49-51.
- Gray, W. M., 1968: Global view of the origin of tropical disturbances and storms. Mon. Wea. Rev., No. 10, 96, 669-700.
- _____, 1971: The magnitude of and the fundamental role of the up-moist and down-dry vertical circulation of the troposphere. Paper presented at Seventh Tech. Conf. on Hurricanes and Tropical Meteor., Barbados, W. I., Dec.
- Gregg, W., 1922: An aerological survey of the United States: Part I, results of observations by means of kites. Mon. Wea. Rev., Suppl. No. 20, 78 pp.
- Hantel, M., 1970: Monthly charts of surface wind stress curl over the Indian Ocean. Mon. Wea. Rev., October, Vol. 98, No. 10, pp. 765-773.
- Hasse, L. (trans. J. F. T. Saur), 1970: On the determination of the vertical transports of momentum and heat in the atmospheric boundary layer at sea. Oregon State University, Department of Oceanography, Technical Report 188, Reference 70-22, August.
- _____, and Wagner, V., 1971: On the relationship between geostrophic and surface wind at sea. Mon. Wea. Rev., Vol. 99, No. 4, April, pp. 255-260.
- Hellerman, S., 1967: An updated estimate of the wind stress on the world ocean. Mon. Wea. Rev., 95, 607-626.
- Hoxit, R., 1972: Dynamics of the Planetary Boundary Layer as Revealed by Observations. Ph. D. dissertation, Department of Atmospheric Science, Colorado State University (in preparation).

- Monin, A., and S. Zilitinkevich, 1967: Planetary boundary layer and large-scale atmospheric dynamics. Stockholm GARP Report. WMO publication.
- Ooyama, K., 1964: A dynamic model for the study of tropical cyclone development. Geofisica International, 4, 187-198.
- Priestley, C. H. B., 1951: A survey of the stress between the ocean and atmosphere. Australian J. Sci. Res., Ser. A, 4 (3), 315-328.
- _____, 1967: On the importance of variability in the planetary boundary layer. Stockholm GARP Report. WMO publication.
- Riehl, H., et al., 1951: The northeast trade of the Pacific Ocean. QJRMS, 77, 598-626.
- Roll, H. U., 1965: Physics of the Marine Atmosphere. Academic Press, New York, 426 pp.
- Sheppard, P. A., H. Charnock and J. R. D. Francis, 1952: Observations of the westerlies over the sea. QJRMS, Vol. LXXVIII, No. 338, October, pp. 563-582.
- Sheppard, P. A. and M. H. Omar, 1952: The wind stress over the ocean from the observations in the trades. QJRMS, 78, 583-589.
- Simpson, J., 1971: A note on the CISK mechanism in the tropics and its role in disturbance formation and maintenance. (unpublished manuscript available from NOAA Miami office).
- World Meteorological Organization, 1967: Stockholm GARP Report. WMO publication.
- Westwater, F. A., 1943: Wind structure over the sea. Weather, 207-213.
- Williams, K., 1970: A Statistical Analysis of Satellite-observed Trade Wind Cloud Clusters in the Western North Pacific. Atmos. Sci. Paper No. 161, Colorado State University. 80 pp.
- Zipser, E. J., 1969: The role of organized unsaturated convective downdrafts in the structure and rapid decay of an equatorial disturbance. J. Appl. Meteor., 8, 799-814.